Thin-film media—Current and future technology

by K. E. Johnson
C. M. Mate
J. A. Merz
R. L. White
A. W. Wu

In the last ten years, the fundamental technology of recording media has evolved from particulate to thin film. The introduction of magnetoresistive heads in 1990 has had further impact on the design of thin-film media. Changes in substrates, magnetic films, overcoats, and lubrication form the basis of the evolution. Design concepts and manufacturing considerations for high-areal-density thin-film disks are described in this paper, with reflections on future enhancements required for media of the next generation.

Introduction

Thin-film recording media of the generic structure shown in **Figure 1** are in general use today in the disk drive industry. The base structure of the disk is an aluminum–magnesium alloy, Al–Mg, that is fabricated to different dimensions depending on the drive size. The most common disk sizes in production are 95-mm diameter with a thickness of 0.8 mm, 65-mm diameter with a thickness of 0.635 mm, and 48-mm diameter with a thickness of 0.635 mm. The aluminum blank is electrolessly plated with an amorphous layer of nickel–phosphorus, Ni–P, with a thickness of 10 μm. The Ni–P-coated disks are abrasively polished, and this is followed by a texturing process resulting in circumferential grooves. Surface finishes can range in root-mean-square roughness, R_q, from 1 nm to 10 nm, depending on the disk application.

The essence of the thin-film disk is the film structure sputtered onto the textured substrate. An underlayer of chromium of thickness 20–100 nm is first deposited to ensure the nucleation of the magnetic film with the easy axis of magnetization in plane. The magnetic film, a cobalt alloy with chromium and coercivity-controlling elements such as platinum or tantalum, is sputtered next. Magnetic thicknesses are as thin as 30 nm for applications with magnetoresistive (MR) heads. A protective layer of hydrogenated carbon of 10–20 nm is reactively sputtered. After emerging from the sputtering tool, the disk is lubricated with several monolayers of a perfluorocarbon lubricant to reduce friction.

This paper reviews in detail the technology that goes into these different layers and suggests directions for thin-film disk technology that will support the areal densities needed for future products.

Thin-film disk substrates and substrate processing

• *Substrate materials*

Substrates are the foundation on which all rigid magnetic recording disks are constructed. During the era of

0018-8646/96/$5.00 © 1996 IBM

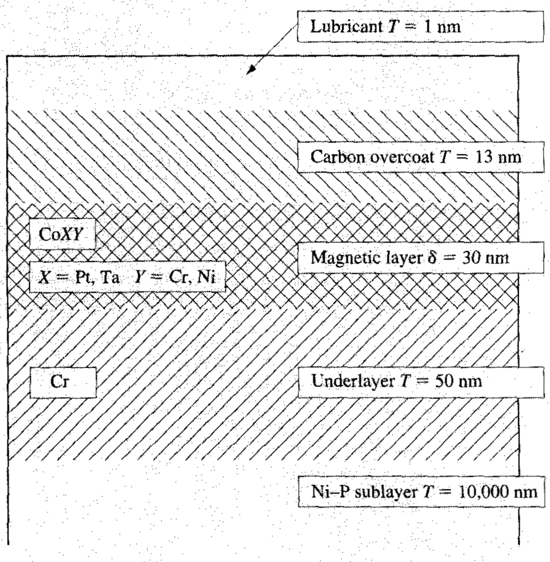

Figure 1

Cross-section structure of a typical thin-film disk.

particulate disk technology from 1955 to 1985, when γ-Fe_2O_3 particles were dispersed in a polymer binder and spin-coated, the substrates used were exclusively Al–Mg, with an anodized aluminum oxide layer.

Thin-film disk technology uses Al–Mg as the base substrate material, but instead of an anodized layer, a hard Ni–P layer is electrolessly plated on the surfaces [1]. The purpose of the Ni–P layer (7–15 μm thick) is to cover up the inherent intermetallic defects of the polished aluminum substrates and to provide a hard surface layer which can be polished to mirror-finish quality. The polished surface is textured in a separate step to add a controlled roughness. The thicknesses and diameters of the Al–Mg/Ni–P substrates have decreased over time to accommodate low-profile drives and to increase volumetric density (the stacking of more disks within a specific form factor).

In addition to reduction of thickness and diameter, further demands are placed on media suppliers. First, disks must be smooth and flat. This allows higher areal densities by permitting the recording heads to fly closer to the disk surfaces. Second, disks must be shock-tolerant in order to allow drive manufacturers to build drives that are more robust and resistant to shock damage.

Because of the relatively low hardness of today's Ni–P/Al–Mg substrate, head–disk impacts can plastically deform and permanently damage the surface, with a loss of recorded data. The threshold for damage has been reported to be below the standard established by the drive manufacturers. Because of the need for thin and flat substrates with high shock resistance, a quest for alternate substrate materials is ongoing.

- *Texturing of substrates*

Overview The texturing operation was added to the thin-film disk process to increase the surface roughness, preventing high static-friction forces between the slider and disk at rest. The surface roughness is also a key parameter determining slider–disk interface durability and minimum head fly-height. Texture also has a strong influence on magnetic performance. Originally it was expected that texture would degrade magnetic performance, but magnetic uniformity and performance can be enhanced in some situations.

Texturing process The texturing process is primarily a mechanical operation in which uniform, controlled scratches are cut into the polished surface of the Ni–P substrate coating (**Figure 2**) to increase the surface roughness. These scratches influence the crystal growth during sputtering of the magnetic film. The pattern of the scratches is important for magnetic performance.

The rosette scratch pattern [Figure 2(a)] is typical for polished substrates, coming from the motion of the commonly used polishing machines. The purpose of these polishers is to remove a small amount of Ni–P, eliminating the plating roughness while improving the desired flatness. The scratches obtained from this process are at acute angles to the recording direction and can cause defect problems. Also, magnetic anisotropy develops along the scratch lines, and the preponderance of radial scratches gives poor magnetic properties in the recording direction.

The circumferential scratch pattern [Figure 2(b)] improves the squareness of the M-H loop due to the magnetic orientation along the scratches. This scratch pattern also gives rise to very low signal readback modulation. Circumferential patterns are obtainable on most commercial texturing equipment.

The crosshatched texture pattern [Figure 2(c)] is produced by the addition of radial motion during the texturing process. The crosshatch is the angle formed by the intersection of the scratch lines. The majority of thin-film disk makers use this crosshatched pattern. One unexpected performance effect is that, although static friction ("stiction") is reduced with the crosshatched pattern, a loss in durability occurs [2, 3].

Texturing methods Two basic process methods for mechanical texturing involve the use of fixed and free abrasives. Both methods use small (less than 5 μm) abrasive particles, such as alumina, silicon carbide, or diamond. The biggest difference between fixed and free processing is the method used to bring the particle to the substrate.

In the fixed abrasive process, the particles are held fixed in a binder that is coated onto MYLAR® tape. The abrasive tape is delivered to the substrate surface and pressure is applied by a compliant roller. A lubricant or coolant is applied to the tape–disk interface. The advantage of the fixed abrasive process is that it has a high stock removal rate, allowing the desired roughness level to be reached more rapidly.

During the cutting operation, the Ni–P material removed from the scratches has a tendency to either adhere along the edge of the scratch or reattach elsewhere. These defects are called "re-welds," or "weldments." There are two issues associated with large scratches. The film growth differences associated with large scratches can cause magnetic defect sites. In addition, the larger scratches have more Ni–P material removed and are more likely to form weldments. To minimize weldment formation, cutting fluids are used. However, the tendency to form weldments remains a disadvantage of fixed abrasive processing, even with the use of the cutting fluids.

In the free abrasive process, the abrasive particles are applied in slurry form. The slurry consists of water, abrasive, cutting fluids, lubricants, and surfactants. The slurry is applied to the disk surface with a cloth or pad material. In free abrasive processing, the particles have the freedom to roll, since they are not held rigidly by a binder. This free abrasive processing is less likely to create deep scratches, but the cutting efficiency is low, so processing times tend to be longer. Free abrasive slurries typically have one or more additives: 1) surfactants to lower the surface tension; 2) cutting fluids or lubricants to minimize weldment formation; and 3) stabilizers to hold the abrasive particles in suspension.

Commercial equipment Two commercial machines are used widely for texture processing. One type can be used for either fixed or free abrasive processing. For free abrasive processing, the slurry is delivered to the disk–cloth interface. The disk rotates as a compliant roller, and each side of the disk applies force to the cloth. The rollers and cloth assembly oscillate radially to yield the crosshatched pattern. The crosshatch angle is controlled by the cloth–roller oscillation amplitude and frequency and the disk rotational speed. The spent cloth is also advanced during processing. A second machine type has free abrasive capability only. Here, the disk is held on a rotating table. A rotating, circular quill with a pad attached applies force to the disk surface as the abrasive is applied. The relative speed of rotation of the quill and disk controls the crosshatched pattern.

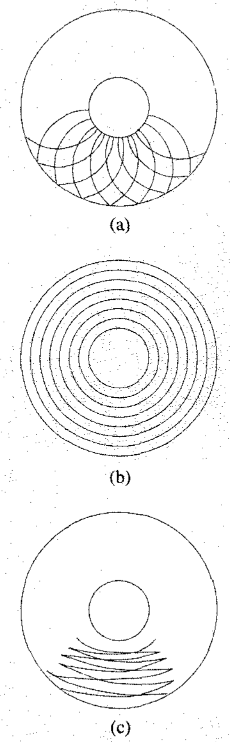

Figure 2

Substrate texture: (a) Radial rosette; (b) circumferential; (c) circumferential with crosshatching.

- *Measurements and characterization*

The surface roughness, R_q, of the texture is the parameter that can be correlated to stiction force between the head and disk at rest, to interfacial durability, and to overall magnetic performance. The ability to accurately quantify roughness is essential. Measurement methods can be broken down into two categories—contact stylus and noncontact optical.

Contact stylus is the most common measurement method for texture roughness. Tencor P-1, Tallystep, and Dektak are three commercially available contact stylus measurement tools. A typical roughness trace occurs with a stylus having a radius of curvature of 0.15–3 μm scanning a length of 0.3–2.0 mm, the order of the slider length. Parameters such as R_q, the root-mean-square roughness, R_a, the arithmetic average roughness, and R_p, the peak height, are measured. Stylus measurements usually have excellent correlation to performance parameters. However, the measurement takes 30 to 100 seconds per scan, and is not suitable for use in a manufacturing setting. Another disadvantage is the small

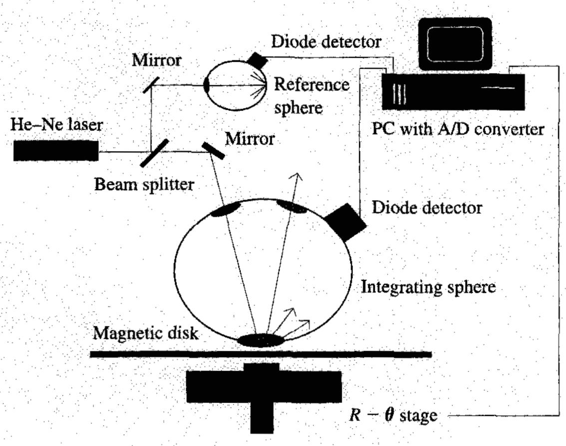

Figure 3

Schematic diagram of Optical Texture Analyzer.

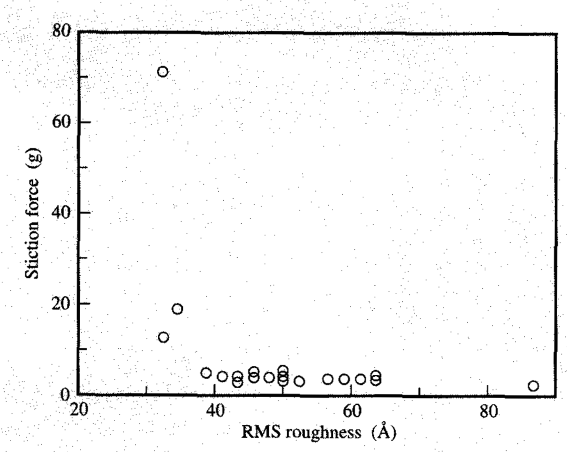

Figure 4

Stiction vs. surface roughness.

amount of disk surface evaluated. It takes many scans to obtain a good representation of the overall surface roughness. Finally, stylus measurements provide only two-dimensional information; in order to estimate the three-dimensional roughness, a second trace orthogonal to the first is required.

Optical methods are typically quicker and also provide information about the three-dimensional surface roughness. The Wyko, Zygo, and MP2000 tools and the IBM Optical Texture Analyzer (OTA) are all in general use. One must exercise care when using optical profilometers that depend on the optical properties of the surface, because this can lead to erroneous surface roughness measurements. Experience has shown that the IBM-developed OTA (**Figure 3**) has provided excellent correlation to stylus measurements and performance. The OTA collects the amount of scattered light from a laser beam into an integrating sphere and quantifies the result [4]. The OTA can measure a track 0.8 mm wide with 360 measurements in 20 seconds, and is thus well suited as a process control tool in a manufacturing environment.

Surface roughness alone does not define disk performance. Scratch uniformity, weldments, and other texture anomalies (e.g., misdirection scratches, haze, scuffs) can be more important than roughness in determining performance. Characterization techniques such as scanning electron microscopy (SEM), optical microscopy, and focused bright light are tools which also provide insight into performance. In addition to these conventional techniques, scanning probe techniques such as scanning tunneling microscopy (STM) or atomic force microscopy (AFM) have been used for high-resolution studies of surfaces [5–8].

- *Manufacturing issues*

Manufacturability is an important factor in designing a texture process. Consideration must be given to several parameters. First, good process control is necessary. The texture process must produce parts for which the variability of the process is much less than the acceptable specification range. Good process control requires reliable measurement tools and the use of statistical process control techniques. Second, cycle time must be minimized. Since disks are textured one disk or side at a time, it is important to keep the process time short to maximize output per texture tool. Finally, cost considerations are important. In addition to the operator cost and machine depreciation, the cost of raw materials used must also be considered.

- *Performance effects*

The texturing of the disk surface affects stiction, friction, durability, head flying height, and magnetic performance. The goal of a texture process is to provide a surface that has very uniform scratches free of high peaks and defects. In general, there is conflict among the various requirements for mechanical performance. For lower stiction forces, higher roughness is desired (**Figure 4**). The effective slider–disk contact area is lowered with increasing roughness, and so is the stiction force. However, as the slider takes off and lands, the wear rate depends upon the contact area. Worse durability is observed at higher roughness (**Figure 5**).

Texture effects on magnetic performance are generally deleterious, increasing missing-bit defects (**Figure 6**) and degrading soft-error rate (**Figure 7**). Smooth surfaces are best for magnetics; surfaces of intermediate roughness are the best compromise for stiction and wear attributes.

- *Recent developments*

Dual-zone texture Because of the conflicting requirements for optimum magnetic and mechanical performance, an obvious process solution is to separate the magnetic data zone from the landing zone. The landing zone can be optimized for the parameters that provide good stiction and durability, and the data zone for magnetic performance.

The issues involved in such a design are

- Small tolerances involved in texture zone placement vs. slider landing accuracy.
- Reliability of the mechanism which returns the slider to the landing zone for emergency power-off situations.
- Flight stability of the slider as it passes from data to landing zone.
- Data storage area lost to the landing and transition zones.
- Additional data zone processing.

The dual-zone texture approach does have the advantage of allowing high flexibility in the preparation of the landing zone. The landing zone surface can be prepared using the mechanical texturing techniques discussed above, but a new approach using laser technology is proving the most versatile [9, 10].

Laser-texture landing zone At IBM, the laser-texturing approach has been adapted for disk manufacturing [10]. The technique employs a high-repetition-rate Q-switched infrared laser whose pulses melt microscopic spots on the Ni–P surface. The laser is focused on a spinning substrate, which also moves radially. The process of shock-melting and resolidification creates an array of protruding microdomes or bumps near the inner diameter (ID) of the substrate. The bumps serve as smooth contact points for the landing slider. Surface tension eliminates any residual substrate roughness in the molten regions.

The laser-texture process involves material redistribution rather than removal; i.e., volume is conserved. Besides simplifying the topography formation (no redeposition), this also eliminates any health-hazard concerns. The bump heights are very reproducible and can be tuned to any height in the range from 0 to 60 nm. **Figure 8** shows an atomic force microscope (AFM) image of an array of such bumps with a center height of 30 nm. Each bump consists of a central dome surrounded by a trough, which in turn is surrounded by a rim of lower height than the dome. The diameter of the rim is typically 15 μm. Slope angles on the bumps are rather small, being less than one degree. (They appear much steeper in a representation such as Figure 8 because of the ~300× expanded vertical scale.) In the example shown, the bumps are spaced 50 μm by 50 μm. Using this technique, landing zones can be created at the disk ID with very high precision at competitive cost. The process also offers environmental and manufacturing advantages because no

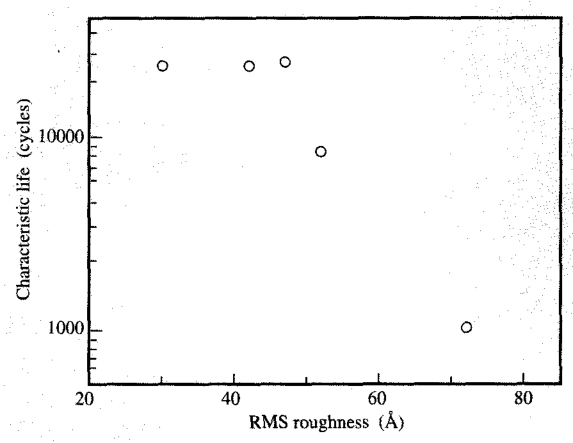

Figure 5

Durability vs. surface roughness.

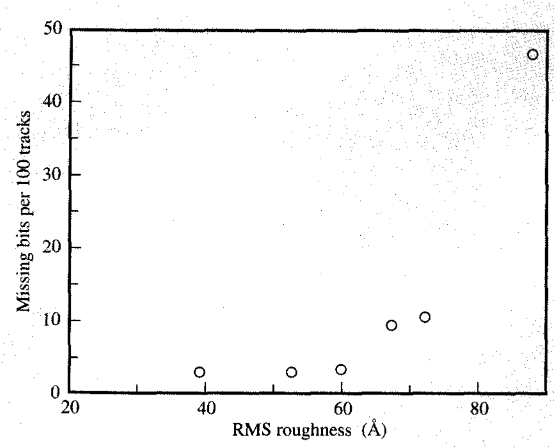

Figure 6

Missing bit density vs. surface roughness.

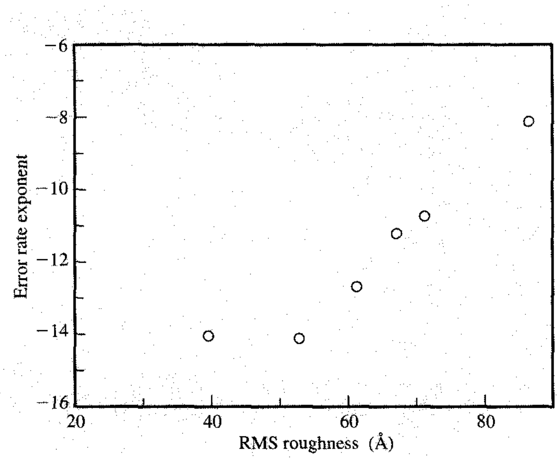

Figure 7

Soft-error rate vs. texture roughness.

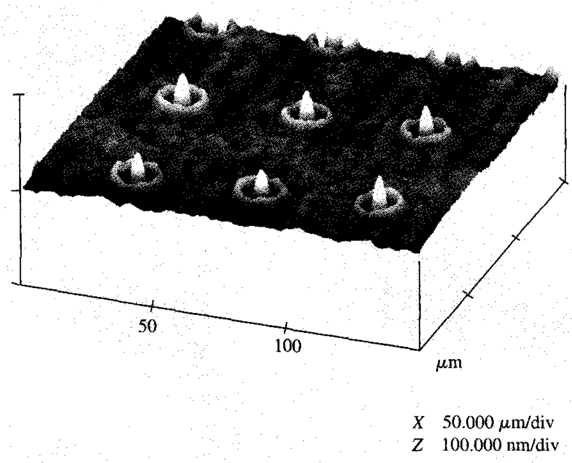

Figure 8

AFM image of an array of laser bumps [10].

solvents are necessary and no chemical discharges arise. Tribological performance in the laser-textured landing zone is excellent. The fact that laser texture, unlike an abrasively textured landing zone, has no difference of mean level between the data zone and the landing zone also eliminates flyability concerns when the slider enters or leaves the landing zone.

Data zone The data zone, in a dual-zone texture structure, may require additional processing beyond standard polishing. One alternative is to process the data zone with low roughness and low crosshatch angle. Another processing option is to polish the surface finely so that it has no discernible scratches or scratch direction. This highly polished surface has the advantage of allowing the sputtering system to dictate magnetic grain growth. In addition, since the surface is scratch-free, the magnetic film can be defect-free.

- *Alternate substrate materials*

Material considerations Currently there are a number of alternate substrate materials available in the industry. The main contenders are chemically strengthened glass, glass-ceramic, and amorphous carbon. Others, such as titanium, silicon, silicon carbide, and beryllium, are also available. A comparison of their physical properties is presented in **Table 1**. For chemically strengthened glass (soda lime and aluminosilicate), the advantages are derived mainly from their stiffness and hardness [11, 12]. They can be polished to a high degree of surface finish and can be microtextured chemically or by other proprietary processes [13–15]. They are less deformable during processing or during clamping, and they can withstand higher shock forces than disks that are produced with Al–Mg/Ni–P substrates. Some of the disadvantages include the potential existence of edge chippings, cracking, and microscopic surface flaws in the glass that may lead to failures when the substrate is subjected to high thermal shock within the sputtering systems or under high rotation speed in the actual drives [16]. Their high heat emissivity (rate of heat loss) can often lead to lower temperatures of magnetic film deposition. This may adversely affect the recording performance from low coercivity and poor signal-to-noise ratio [17]. Static charging after an aggressive cleaning can often lead to a contamination problem by attracting airborne particles. It is, however, difficult to dispute the fact that media fabrication technology on glass substrates is well established [18–24] and that glass disks are finding applications in the storage industry.

Glass-ceramics have also been considered as disk substrates [25, 26]. They are stronger and tougher than glass and are less sensitive to damage. Their fracture strength is several times higher than that of conventional glass. One of the important advantages of glass-ceramics is believed to be their inherent surface roughness, which requires no additional texturing to achieve a good contact start/stop (CSS) performance. The degree of texture can be controlled by varying the crystal size and the polishing process. On the other hand, there are small pits often associated with this natural surface roughness. This may or

Table 1 Comparison of alternate substrate materials.

Material	*Density* (g/cc)	*Modulus* (GPa)	*Yield strength* (MPa)	*Thermal exp.* (10^{-6}°C)	*Thermal cond.* (W/mK)	*Usable temp.* (°C)	*Hardness* (kg/mm^2)
Ni–P plated	2.7	72	117	24.2	80.0	280	500
Soda glass	2.5	75	37	8.5	0.75	500	540
Al–Si glass	2.5	85	—	9.1	2.0	500	590
Glass-ceramic	2.7	83	>200	12.0	1.3	>500	650
Carbon	1.8	35	90	3.0	10.0	2500	650
Silicon	2.3	190	—	3.5	120	1400	1000
SiC	3.2	460	400	4.5	250	1650	2500
Be	1.8	303	350	12.0	200	280	150
Ti	4.5		276	8.4	220	1670	435

may not have an impact on the recording performance, depending on the areal density that is required for the finished disks. The pit dimensions can be reduced if the ceramic is glazed with a glass layer and polished, or by coating with a planarizing polymer [27]. Like glass substrates, glass-ceramics also suffer the disadvantages of high heat emissivity and surface charging due to their electrically insulating properties.

Carbon is another viable substrate candidate that may satisfy many of the requirements for high-density recording [28, 29]. It is inherently light (density = 1.8 g/cc) when compared to the other substrates. This can be an advantage with regard to battery power consumption by the spindle motors in compact drives. Its high surface hardness may lead to better shock resistance against head slap caused by external acceleration. Unlike glass and glass-ceramic, carbon is electrically conductive. There is no static charge buildup on the surfaces that can lead to particle contamination problems during processing. Another advantage of carbon is its high heat resistance, which allows higher sputtering temperatures for the magnetic film deposition. Processing of carbon through vacuum deposition systems is also simpler, since it is more compatible with the process that is currently dedicated to the Al–Mg/Ni–P substrates.

There are a few disadvantages associated with carbon substrates. First, the material is fragile and subject to breakage when not properly handled. Second, texturing of carbon is still under development and will require some additional improvements before it can be implemented.

Other substrates such as titanium, silicon, silicon carbide, and beryllium are also available, but only in small quantities. A close examination of their physical properties reveals that there are merits and weaknesses for each of these substrates. It is also fair to say that the quality of these substrates is evolving as suppliers improve their manufacturing processes. It is important to remember that the final selection of any particular substrate must depend not only on its physical properties, but on other considerations such as ease of cleaning and sputtering, process compatibility with Al–Mg/Ni–P substrates in order to avoid any major impacts on existing manufacturing lines, potential flatness or curvature degradation after processing, texturability, cost, and availability.

Alternate substrate texturing issues The texturing of glass substrates can be done mechanically using diamond slurry or chemically by means of etching. Both of these techniques should be performed prior to the mechanical strengthening process because of concerns about creating sites which could lead to crack propagation. Photolithography, sol gel, and material deposition through a mask are well suited to alternate material substrates [3]. The transient metal underlayer (TMU) process developed by IBM is another technique that is well suited for alternate substrate materials [30]. TMU utilizes low-melting-point metals, such as Ga, deposited on a nonwetting substrate. The substrate is held above the melting point of the metal. The deposited metal balls up and forms liquid islands. The subsequent deposition of the magnetic and carbon films maintains the roughness topography from the island topography. This surface topography lowers stiction by reducing the slider–disk contact area.

Magnetic media developments

• *Overview*

The magnetic design of rigid-disk magnetic media has changed fundamentally in the last decade. The use of magnetic oxide particles as the source of magnetic flux has been replaced by the use of magnetic thin films. The switch from magnetic oxides to magnetic metal films was driven by the requirement for films with high saturation

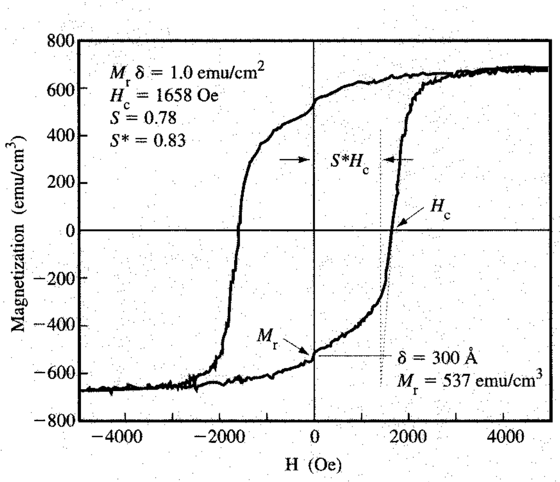

Figure 9

M-H curve of thin-film disk suitable for readback with MR head.

magnetization, M_s, and very low thickness, δ, to achieve high recording densities. The use of thin-film technology integrates a new set of magnetic, materials science, and manufacturing challenges. The major magnetic issue that has emerged is the reduction of intrinsic media noise that, with the use of MR heads, competes with other system noise sources to limit areal densities. Development of thin-film materials for low-noise applications has been quite successful on the basis of improved understanding of the nanostructures of thin-film disk materials. The deposition of thin-film disk layers can be done by several techniques, but is now almost universally done by the sputtering process. The interrelationship of magnetic materials and magnetic recording properties, film microstructures, and process effects has resulted in thin-film disks capable of 500 Mb/in.^{2} in the marketplace and projections of 10 Gb/in.^{2} in the next ten years. This section discusses the magnetic and recording properties of today's thin-film disks and the structures that are necessary to accomplish these goals.

- *Magnetic properties*

Rigid-disk-media magnetic properties can be conveniently subdivided into macroscopic and microscopic properties. An understanding of each is needed to design thin-film media for the desired signal-to-noise ratio, S/N, required by the magnetic recording system. Macroscopic properties such as coercivity (H_c), remanence-thickness product ($M_r\delta$), coercive squareness (S^*), and squareness (S) determine readback signal variables such as pulse shape, amplitude, and resolution. These disk parameters are indicated in **Figure 9**, which shows an M-H hysteresis curve taken with a vibrating sample magnetometer (VSM) of a thin-film disk suitable for readback with an MR head. Microscopic properties such as grain size, grain coupling, and grain crystallographic orientation determine the noise properties of the films. An optimization of macromagnetics for signal and micromagnetics for noise is necessary to produce the optimum disk.

Macromagnetics Theoretical work was presented in 1971 by Willams and Comstock that allows one to calculate recording responses of media knowing H_c, M_r, δ, and S^* in conjunction with head fly height d and head gap length g [31]. From their analysis, the Williams–Comstock parameter, a, has been derived that relates macromagnetic properties of a disk and field distribution of an inductive recording head to isolated pulse widths. The original expression has been simplified to the following, assuming S^* values close to 1 [32]:

$$a = \left\{ \frac{4M_r\delta[d + (\delta/2)]}{H_c} \right\}^{+1/2}. \tag{1}$$

Combining this factor with the formula for pulse width at 50% amplitude,

$$PW_{50} \cong \sqrt{g^2 + 4(d + a)(d + a + \delta)}\,, \tag{2}$$

one can approximate the readback voltage for any head–disk combination. The analysis has to be modified only slightly for the use of MR heads. The general design criterion for rigid disk media is to minimize PW_{50} and a by increasing the coercivity H_c as much as possible without exceeding the writability of the head, keeping S^* high for narrow switching field distributions leading to narrow transitions, and keeping δ very low for high-frequency output and to preclude MR head saturation. M_r must be adjusted to give adequate signal output without sacrificing resolution.

A thin-film disk is the preferred recording medium to satisfy these requirements. High H_c is easily attained in thin-film disks by using appropriate Co ternary and quaternary metal film alloys. Values in use today are between 1500 and 2000 Oe. The potential for H_c greater than 3000 Oe has been demonstrated [33]. High S^* values are desirable to achieve small a values. S^* values are large and consistently greater than 0.8 in thin-film media because of strong coupling in the grain structure. As is discussed later, S^* values above 0.90 may not be desirable, since they are often indicative of high noise.

Signal parameters related to thin-film macromagnetic properties are typically measured on every manufactured disk on specially designed recording test stands. Signal amplitudes are measured at two frequencies, and the resolution, defined as the ratio of the two amplitudes, is carefully monitored. Signal dropouts occur from surface and film defects; if the number and extent of the dropouts are significant, the disk is rejected.

Micromagnetics Thin-film media are composed of grains between 100 and 500 Å in diameter. As seen in the transmission electron micrographs of **Figure 10**, the grains can be very close together, leading to strong magnetostatic and intergranular exchange interactions. The exchange forces are ignored in particulate media, but are of ultimate importance in thin-film media. During the magnetic recording process, exchange interactions cause the grains to act cooperatively. In a dc-erased state, the magnetization direction over a large scale is constant; dc-erase noise is low in thin-film media. On the other hand, when one investigates the actual transition region between oppositely magnetized regions in a recorded track, more chaotic behavior is observed. Zigzag walls or sawtooth transitions are observed. The wall is irregular across the track width, and this nonuniformity in the zigzag leads to noise in the transition.

The consequences of having highly coupled thin films with zigzag walls in the recorded transition were demonstrated in the 1980s [34]. Noise power in thin-film alloys of CoNi, Co, and CoRe was investigated to densities of 1500 fc/mm, as shown in **Figure 11**. The noise power increases with recording density. The key development that has occurred for the extendibility of thin-film media is an understanding of how to minimize exchange interactions through microstructural modifications, giving a low-noise medium while at the same time keeping the macromagnetic properties within the desired ranges.

The noise content of thin-film media is monitored in several ways. Disk drives are specified to a bit error rate, and this is strongly influenced by the media noise. This is a complicated measurement done either at the drive level or on sophisticated magnetic recording test stands. More conventional measurements are done on simpler test stands where noise and/or peak jitter assessments can be made. With the use of MR transducers, thin-film disk media noise is becoming the major noise contributor in the disk drive, and the measurement and subsequent reduction of media noise are extremely important.

- *Fabrication of thin-film media for low noise*

The following sections discuss the microstructures necessary for low-noise thin-film media and the techniques in general usage to minimize interactions and noise.

Physical grain segregation Physical grain segregation has been observed in TEM micrographs in low-noise thin-film media, as seen in Figure 10. There are several means to achieve voided grain structures within the control of the thin-film disk fabricator.

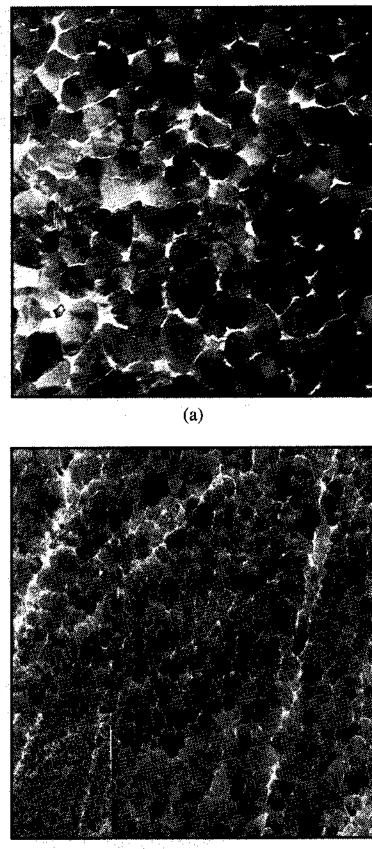

(a)

(b)

Figure 10

TEM micrographs of two different magnetic films.

Process effects Sputtering process effects on thin-film disk microstructure and media noise have been interpreted using adatom mobility arguments initially put forth by Thornton [35, 36]. **Figure 12** shows a zone diagram for metal films deposited by magnetron sputtering showing the effect of temperature and sputtering pressure on film structure. T is the substrate temperature, and T_m is the melting point of the thin-film material. Sputtered films deposited at low temperatures and high pressures fall into Zone 1 and exhibit a columnar growth structure defined by voided open boundaries. Voided grain structures are desired for low-noise media. Low sputtering rates, high sputtering pressure, low sputtering temperatures, and the absence of bias are low-mobility sputtering conditions that rob the sputtered atoms of their kinetic energy during atom transport and film growth, allowing the formation of the voided structures.

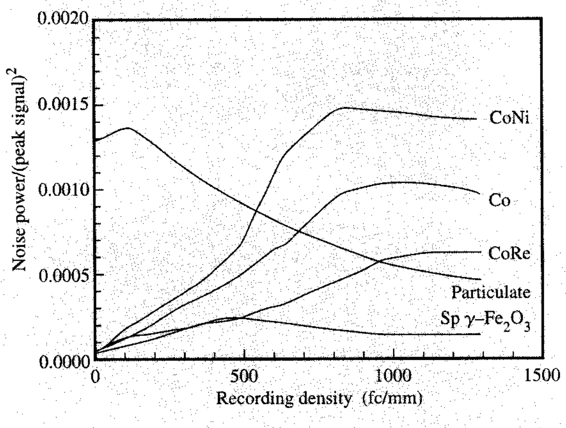

Figure 11

Normalized medium noise vs. recording density for various media [34].

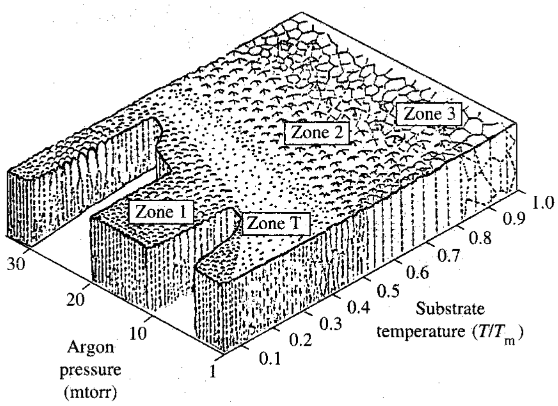

Figure 12

Microstructure zone diagram for magnetron sputtered films [35]. T = substrate temperature; T_m = melting point of the coating material.

Underlayer effects The use of underlayers is universal in the fabrication of thin-film media. Their primary purpose has been to nucleate magnetic films with the c-axis in-plane or nearly in-plane to produce high-H_c and high-squareness magnetic films. It is now clear that the nature of the underlayer also has a large effect in determining noise performance. Magnetic films tend to replicate the underlayer structure below. Thus, forming segregated underlayer structures should lead to segregated magnetic film structures. Work by Yogi et al. and Natarajan and Murdock in 1988 revealed the reduction of noise with increasing Cr thickness for sputtered films of CoP and CoNiCr [37, 38]. It is observed that Cr underlayer grains enlarge and segregate with increasing thickness and propagate these properties to the magnetic layer.

There are certain drawbacks in using the underlayer thickness method to reduce noise. First, thick Cr underlayers require more sputtered material and will decrease disk throughput in a disk manufacturing plant. Second, thicker Cr inevitably increases H_c and decreases S^* through the breaking of exchange coupling. Thus, certain macromagnetic designs may not be attainable with a low-noise restriction. Third, lowered S^* values may be indicative of less coupled and quiet films, but low S^* can also have an impact on the recording signal and writability. Finally, for many cases, the noise sensitivity to Cr thickness is not very strong, and only several dB can be gained for rather large Cr thickness increases. Clearly, other noise-reduction techniques are desirable for the optimization of macromagnetic and micromagnetic properties.

Compositional segregation Compositional segregation of grains in thin-film disks is another effective way to minimize interactions, giving low-noise disks. Experimental evidence showing the reality of compositional segregation has been obtained using X-ray fluorescence (XRF) and wet-etching techniques. **Figure 13(a)** shows a structure of Cr precipitation to the grain boundaries consistent with the TEM/XRF mapping work by Chapman and Rogers [39, 40]. Similar Cr enrichment has been observed for ternary CoPtCr films [41]. Wet-etching work by Maeda has led to a slightly different interpretation of the microstructure [42]. In this technique, Co regions are preferentially dissolved, leaving patterns designated as CP (chrysanthemumlike pattern) structures. **Figure 13(b)** shows a CP grain model where each magnetic grain shows internal composition fluctuations [42]. A slightly different internal structure that may be consistent with the chrysanthemum patterns has been observed by Nolan and Sinclair [43]. Multiple small Co grains are clustered on a larger Cr underlayer grain, as shown in **Figure 14.** Neighboring Co grains on the single-crystal Cr grain exhibit a 90° in-plane misorientation consistent with the two directions in which a Co c-axis could epitaxially match the Cr grain. The intergranular region between Co grains has yet to be analyzed by the authors, but could be the Cr-rich alloy described by Maeda.

Other techniques have lent credence to the hypothesis that Co-based magnetic thin films are not compositionally homogenous. As early as 1985, ferromagnetic resonance

(FMR) studies showed the presence of several magnetic constituents in a set of CoCr films [44]. More recently, ferromagnetic resonance studies have been applied to longitudinal thin films, suggesting the formation of Cr-rich nonmagnetic components. Mossbauer studies were performed on CoCr films containing a small amount of Fe [45]. One of the two features observed in the spectrum was identified as a nonmagnetic phase of nearly pure Cr. Recent Brillouin spin-wave scattering studies on CoNiPt films also indicate elemental segregation [46].

Experimental methods for producing compositional segregation Recognition of the macromagnetic differences in M_s compared to the bulk alloy in constant-composition sputtered CoCr perpendicular thin films deposited at different temperatures initiated speculation that composition segregation could occur in thin films. Deviations from the bulk are attributed to the compositional inhomogeneity of the Co and Cr in the grain [47]. The effect of substrate temperature and Cr alloy concentration on sputtered CoPtCr/Cr longitudinal films has been recently reported [48]. High Cr content and higher temperatures lead to lower-noise films, and it is speculated that these variables accelerate the Cr segregation to grain boundaries, forming nonmagnetic phases.

Coupled very closely with the temperature variable, as a means to initiate compositional segregation, is the selection of the alloy and the understanding of its phase diagram [48]. Choosing an alloy composition that can undergo a phase change or a spinodal decomposition at elevated temperatures is necessary to induce compositional segregation. On the basis of equilibrium phase diagrams, it is suggested that certain binary and ternary alloys can be two-phase alloys. Noise performance is better using the alloys that allow two phases such as CoCr and sputtered CoP [38]. Such phase separation may be particularly true for the CoCrTa alloy. Above 2% Ta, the H_c value drops precipitously, suggesting that the hexagonal close-packed (hcp) phase of this composition becomes unstable and that the precipitation of a different phase may be starting [49]. Compositional segregation may help explain why CoCrTa alloys [Figure 10(b)], often lacking any evidence of a physically voided structure, are less noisy than other ternary alloys used for longitudinal recording [50].

The sputtering of quaternary alloys is proving to be an effective avenue to producing low-noise thin-film media, particularly films containing B. It is postulated that the low solubility of B in the Co alloy leads to composition segregation of the "grains" [51]. Fabricating new alloys with constituents having limited solubilities may be the key to the next generation of low-noise alloys.

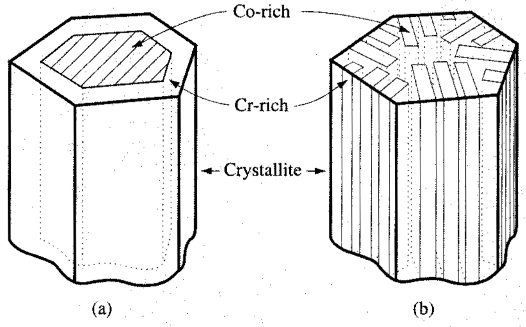

Figure 13

Segregated microstructure models of CoCr perpendicular films [42]: (a) conventional and (b) CP structure model. The CP structure has been observed in longitudinal CoPtCr films.

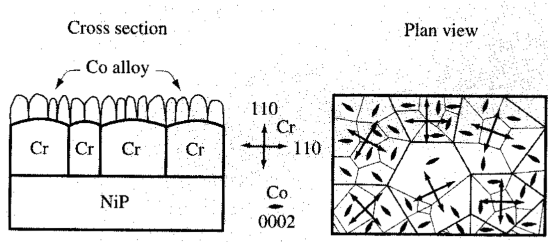

Figure 14

Bicrystal structure showing multiple magnetic grains on a single underlayer grain [43].

Multilayers There has been much interest recently in the use of magnetic multilayers as a means of decreasing noise in thin-film media. By depositing two or more magnetic films separated by a thin nonmagnetic material, noise enhancements have been observed. **Figure 15** shows a schematic cross section of a typical bilayer disk with a nonmagnetic Cr interlayer.

The noise equation for a two-layer disk can be presented as

$$N_T^2 = N_1^2 + N_2^2 + 2\langle N_1 N_2 \rangle , \qquad (3)$$

where N_T is the total noise voltage for the entire structure, and N_1 and N_2 are the individual noise contributions from the separate layers [52]. The magnitude of the noise in each individual layer and the disposition

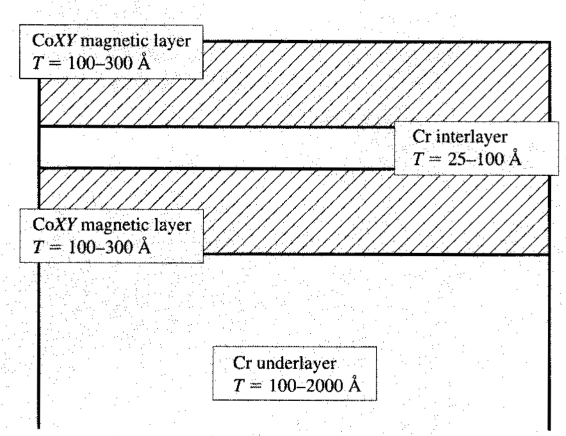

Figure 15

Schematic section of a multilayer thin-film disk.

of the cross term dictate the total noise quantity. Fabricating the multilayered structure with intrinsically quiet single layers is the first step to ensuring a quiet multilayered media structure.

But more important than the low-noise-layer constituents is the nature of the cross term in Equation (3). For a fully coupled structure, exchange coupling will dominate and align the moments parallel in the two layers. The cross term will be positive and equal to $2N^2$, and no noise reduction will be realized. If exchange and magnetostatic coupling are eliminated, the random nature of the interactions will cause the cross term to go to zero because the noise sources would be statistically uncorrelated. Noise will be reduced because the number of grains per unit volume is increased. If the nonmagnetic interlayer is thick enough to break off the exponentially decaying exchange forces, yet small enough to allow for significant magnetostatic interactions, the cross-correlation term can be negative, resulting in even more noise reduction.

- *Areal densities of 10 Gb/in.²*

The advent of low-noise thin-film media along with MR heads in the last ten years has allowed recording areal densities to increase by about 30 times, to 500 Mb/in.² in products and 1–3 Gb/in.² in the laboratory [53, 54]. It is believed that 10-Gb/in.² densities will be achieved in products by 2010 [55]. Accomplishing this goal will require advances in thin-film recording media, MR heads, and electronic channels. The media variables that will make this feat possible are surfaces allowing small head–medium spacings, increased H_c and lower $M_r\delta$ values, and a continuation of media noise reduction. The need for small head–medium spacings is clear from Equation (2). Of any variable, d has the largest effect on PW_{50}. Reduced spacings eventually leading to contact recording require improvements in surface-finishing technologies and inventions in overcoat and lubrication technologies. The use of load/unload transducers may help alleviate the head–media stiction and durability problem. The need for higher H_c and lower $M_r\delta$ values is evident from the Williams–Comstock parameter [Equation (1)]. High-H_c media using thin-film sputtering techniques are thought to be achievable by using CoPtCr and SmCo-type alloys [33, 48]. Media noise-reduction techniques will proceed along one of three paths outlined above.

A concerted effort to understand specific 10-Gb/in.² media requirements has been underway since 1992. Murdock has modeled media macromagnetic requirements for different assumptions of bpi (bits per inch) and tpi (tracks per inch) for the 10-Gb/in.² case [55]. $M_r\delta$ values from 0.35 to 1.0 emu/cm² with corresponding H_c values from 4500 to 2500 Oe are necessary for tpi cases ranging from 11 ktpi to 40 ktpi. The microstructural description of this medium would follow scaling trends using today's conventional wisdom. The media would be composed of small uniform grains with an average diameter of 8–10 nm. For optimum noise, the particles must be completely isolated from one another to eliminate the exchange interaction. Murdock's proposed medium will resemble a densely packed particulate medium.

A limitation to such a medium description is the low S and S^* values that result from particles having no exchange coupling. A low-squareness hysteresis curve results in poor signal output, broadened transitions, and poor overwrite. Min and Zhu have proposed that the optimum medium is one based on a bicrystal structure [56] first described by Mirzamaani et al. [57] and shown schematically in Figure 14. The specific disk structure for high-density recording requires an extension and modification of the current observed bicrystal structures. A preferred orientation of the (100) Cr underlayer will cause the Co magnetic film to grow with $(11\bar{2}0)$ planes parallel to the disk surface and the c-axes on each single-crystal grain aligned either parallel or at 90° to one another in a random fashion. In addition to the crystalline anisotropy along the c-axes, an additional anisotropy is introduced in the bicrystal structure at 45° to the c-axes. The magnetic properties along the effective easy axis are improved, with S and S^* values in the 0.8 to 0.9 range. The more square hysteresis properties can be obtained in conjunction with very low noise [58]. The challenge in creating such a medium is to have the effective easy axis circumferentially oriented.

Whether the 10-Gb/in.^{2} medium is particulatelike or bicrystalline, the grain sizes must be small, with diameters less than 10 nm; this leads to a consideration of superparamagnetic effects. A sufficiently small particle is subject to thermal demagnetization, and below a critical diameter in the superparamagnetic regime, it spontaneously demagnetizes. For a single-layer magnetic film to be marginally stable, the ratio of anisotropy energy $K_u V$ to thermal energy kT must be greater than 60 [59]. For grain thicknesses and diameters ≤ 10 nm, this implies H_c values in excess of 3000 Oe, with specific values depending on M_s.

The introduction of thin-film media into disk drive technology in the last decade has been pivotal in the huge areal densities realized. The technical challenges of media noise reduction and the manufacturing challenges of introducing sputtering technology have been overcome. The next decade will see a continued evolution of thin-film disk technologies.

Overcoats for thin-film media

- *Background*

Slider–disk contact during the operation of head disk assemblies is practically unavoidable. Most commonly, it occurs during each shutdown of the disk file system as the air bearing of the slider is lost during disk spin-down. However, even in disk files with slider load/unload mechanisms, the slider can occasionally apply potentially damaging tractions to the disk surface. For this reason all of the currently used thin-film disks employ a protective overcoat for the magnetic storage layer.

While the primary function of the disk overcoat is to provide wear resistance, especially during intermittent start/stop contact with the ceramic slider, many of the other components of the disk can influence wear performance. Both the underlying topographical texture and the topical lubricant are especially important contributors to disk durability. Development of a mechanically reliable thin-film disk fundamentally involves the study of the interaction among these three parameters—the disk overcoat, texture, and lubricant.

Natural candidates for disk overcoats would be the hard transition-metal oxides, carbides, and nitrides which have been employed in the tool and die industry to improve wear resistance. These films typically must be deposited at temperatures exceeding 400°C to obtain the desirable crystalline structure. Most thin-film disks today are fabricated on Al–Mg substrates which have been electrolessly plated with approximately 10 μm of amorphous Ni–P. In the amorphous state, this hard underlayer is nonmagnetic. However, at temperatures exceeding 300°C, a crystalline magnetic Ni phase rapidly develops which greatly interferes with the magnetic recording process [60]. For this reason, the deposition temperature for today's thin-film disks is limited to approximately 250°C. Given this limitation, few of the refractory compounds have been successfully employed, although thin-film disks have been introduced with ZrO_2 and SiO_2 overcoats [61, 62].

By far the predominant overcoat in the thin-film disk industry is carbon-based. Aisenberg and Chabot [63] used carbon ion beams in their original demonstration of the "diamondlike" properties which can be obtained in deposited carbon thin films. King [64] later demonstrated that desirable disk overcoat properties can be obtained by using a sputter deposition process, which is much more amenable to large-scale disk manufacturing. Because of the wide range of potential applications, the properties of "diamondlike carbon" (DLC) and methods for its deposition have been widely studied and reviewed [65–67]. Notable developments for the thin-film disk industry have been the introduction of hydrogenated overcoats by sputtering carbon films in the presence of H_2 [68] and hydrocarbon dopants (CH_4, C_2H_2, and C_4H_{10}) [69]. In addition, plasma decomposition techniques (plasma-assisted chemical vapor deposition) have been used to deposit DLC films directly from hydrocarbon precursor gases [70–72]. By using similar plasma-deposition techniques, the actual crystalline diamond phase can be obtained with reasonably high rates [73]. Currently these diamond deposition processes require temperatures which are incompatible with the Ni–P underlayers and thus have not found application in the disk drive industry.

- *Properties of carbon overcoats*

The diamond phase of carbon consists of an fcc lattice of carbon atoms, each of which is tetrahedrally bonded (sp^3 hybridization) to four neighboring atoms through strong covalent bonds. The resulting diamond phase has the highest atom density and hardness of any of the materials known to man. The graphitic form of carbon arises from a different type of bonding orbital hybridization (sp^2), which produces three strong planar bonds. The resulting hexagonal lattice is highly anisotropic, with little strength between the parallel planes which contain the threefold sp^2-bonded atoms. In contrast, the DLC films are amorphous, having no long-range crystalline order. As **Table 2** indicates, these amorphous carbon films, deposited both with hydrogen-containing dopants (a–C:H) and without hydrogen (a–C), have properties which can span the range from graphite to diamond.

A wide range of characterization techniques have been employed to probe the details of the structure of the a–C:H films. The consensus that has arisen from these studies is graphically represented in **Figure 16**. This random structure consists mostly of carbon atoms which are bonded to one another with either fourfold (sp^3) or

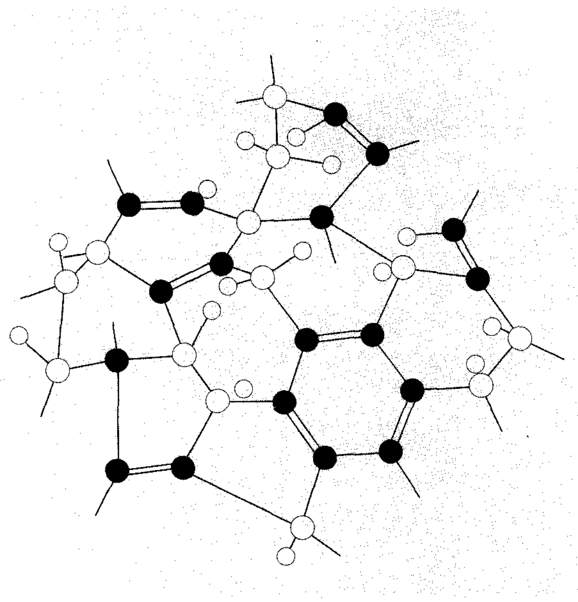

Figure 16

Two-dimensional representation of a proposed structure for diamondlike carbon. Crosshatched circles = sp^3, dark circles = sp^2 carbon atoms, blank circles = hydrogen atoms. Nominal hydrogen atom fraction is 0.33; nominal fraction of carbon sites with sp^3 coordination is 0.28.

Table 2 Properties of various forms of carbon.

	Density (g/cm^{-3})	*Hardness* (GPa)	*sp^3* (%)	*H* (at. %)	*Gap* (eV)
Diamond	3.515	100	100	—	5.5
Graphite	2.267		0		−0.04
C_{60}			0	0	1.8
Glassy C	1.3–1.55	2–3	≈0		0.01
a–C, evaporated	1.9–2.0	2.5	1		0.4–0.7
a–C, mass-selected ion beam	3.0	30–130	90 ± 5	>9	0.5–1.5
PD a–C:H, hard	1.6–2.2	10–20	30–60	10–40	0.8–1.7
PD a–C:H, soft	0.9–1.6	<5	50–80	40–65	1.6–4
Polyethylene	0.92	0.01	100	67	6

threefold (sp^2) coordination. Although controversial, there is clear evidence that graphitic microcrystals can exist in these films under certain growth conditions or postdeposition treatments [74, 75]. Hydrogen in the films partially passivates dangling carbon bonds within the films [76]. It also has the effect of substituting for carbon–carbon bonds, leading to a reduction in the three-dimensional rigidity of the structure.

Because Raman spectroscopy directly probes the lattice vibrational states, it has proven to be a very useful technique for studying the structure of a–C:H films. **Figure 17** illustrates the Raman spectra for diamond, graphite, microcrystalline graphite, and a typical a–C:H film. The deconvolution of the broadened a–C:H spectra resembles the microcrystalline graphite spectra. The additional peak in the microcrystalline spectra results from the breakdown of wavevector conservation rules imposed by long-range crystalline order. Even though the observed Raman scattering is thought to originate from the sp^2-bonded carbon within the a–C:H films, modeling of the Raman scattering process indicates that the presence of sp^3-bonded regions of the carbon films influences the Raman spectra. Specifically, the position of the ≈1580-cm^{-1} G peak shifts to lower wavenumber with increasing sp^3 bond fraction [77, 78]. The relative intensities of the 1320-cm^{-1} D peak and G peak are dependent on the size of any graphitic microcrystals that are present in the film. This relationship between the $I(D)/I(G)$ ratio is not expected to be monotonic. It has been proposed that $I(D)/I(G)$ increases with increasing crystallite size up to crystallites of size 12 Å, and thereafter decreases with increasing crystallite size [79]. In addition, the frequency shift of the G peak with increasing sp^3 coordination is predicted only when crystallite sizes are below the 12-Å size. These sizes of microcrystals begin to stretch the definition of the crystalline phase. Recent studies suggest that the observed Raman data and electrical resistivity data are consistent with aromatic rings containing as few as 4–8 carbon atoms [80].

Nuclear magnetic resonance (NMR) is another powerful characterization technique which, because it is sensitive to the electronic environment of the atomic nucleus, provides direct information about the fraction of sp^3 versus sp^2 C–C bonding. The technique would be more widely applied except for the relatively large amounts of material that are required for analysis (5–10 mg). Nevertheless, C^{13} studies have demonstrated that the sp^3 bonding fraction for a–C:H films typical of disk overcoats ranges from 5 to 15% [81].

The DLC films have been found to be chemically inert and do not decompose even when exposed to strong oxidizing conditions such as concentrated acids. This property and the high electrical resistivity that can be achieved with a–C:H films contribute to the excellent corrosion resistance that is exhibited by current-generation thin-film disks.

The electrical resistivity of these films increases exponentially with increasing hydrogen content [82]. The observed temperature dependence of the resistivity is consistent with a hopping conduction mechanism for amorphous semiconductors, in which electrons tunnel between localized conducting states in the bandgap. The presence of the hydrogen is expected to increase the degree of sp^3 bonding, thereby decreasing the density of localized conducting states associated with sp^2-bonded carbon.

The optical properties are intimately related to the electrical properties—higher electrical resistivity is associated with larger optical bandgaps. Optical absorption has generally been found to obey the Tauc relation for amorphous semiconductors [83],

$$\sqrt{\alpha \hbar \nu} = G(\hbar \nu - E_g), \quad (4)$$

where α is the linear absorption coefficient, $\hbar$ is Planck's constant, ν is the photon frequency, and E_g, the optical bandgap. In contrast to the crystalline diamond films, some absorption is observed below the bandgap energy due to the localized states that exist in the bandgap, as discussed above. The films nevertheless have excellent IR transparency and have found application as antireflective coatings for IR sensors.

The mechanical properties of DLC films are of particular interest because they are directly related to their tribological performance. Specifically, classical wear theory predicts that wear resistance should be proportional to the hardness of the films [84]. As indicated in Table 2, mass-selected ion beam deposition techniques can produce films with very high fractions of sp^3 carbon bonding and hardness which equals that of diamond. Relatively high ion energies (>50 eV) are necessary to promote the sp^3 bonding. The density, hardness, and elastic stiffness all scale with increasing fractions of sp^3 bonding because the higher coordination number relative to sp^2 bonding leads to a more rigidly constrained structure.

For the lower-energy sputter deposition processes used for thin-film disk overcoat deposition, it has been found that the presence of atomic H in the films promotes the sp^3 carbon bonding. This process is essential to the generation of crystalline diamond films, because H stabilizes the surface sp^3 hybridization. Diamond-phase growth then occurs as carbon atoms are substituted for hydrogen atoms on surface C–H bonds. In the a–C:H films sputtered with H_2 or hydrocarbon dopants, considerable C–H bonding can remain in the films. As **Figure 18** indicates, incorporation of hydrogen can lead to a decrease in hardness as the terminating C–H bonds reduce the rigidity of the film structure. Raman scattering data in combination with film hydrogen content can be used to quantify this trade-off between the competing effects of C–H bond termination and C–C bond structural rigidity. In addition, a–C films sputtered in argon only can be made with a wide range of density and hardness depending on sputter deposition power and pressure [85, 86].

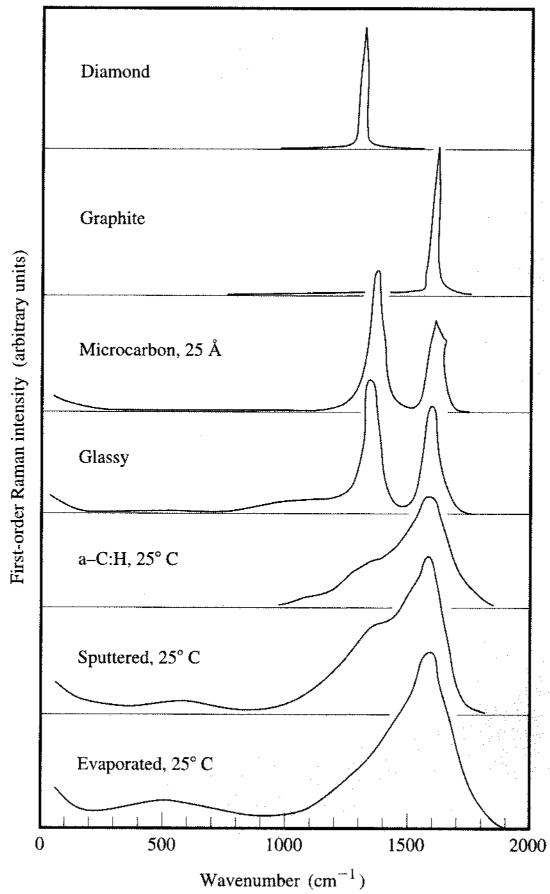

Figure 17

First-order Raman spectra for various types of carbon.

The intrinsic deposition stress present in these films is often highly compressive and correlated to hardness. Stress levels can be so high (>4 GPa) that they can limit the maximum thickness to which the films can be deposited [87]. As the films grow thicker, the stored elastic strain energy builds to a critical level and causes film delamination from the substrate. The stress levels present in the PECVD films have been found to depend on the hydrocarbon dopants and can be reduced by additions of N_2 in the plasma [88, 89].

- *Wear mechanisms and their relation to disk film performance*

The thin-film disk overcoat has two primary functions. Foremost, it must prevent any wear of the magnetic layer and subsequent data loss. This function must be accomplished with a minimum of debris generation, which

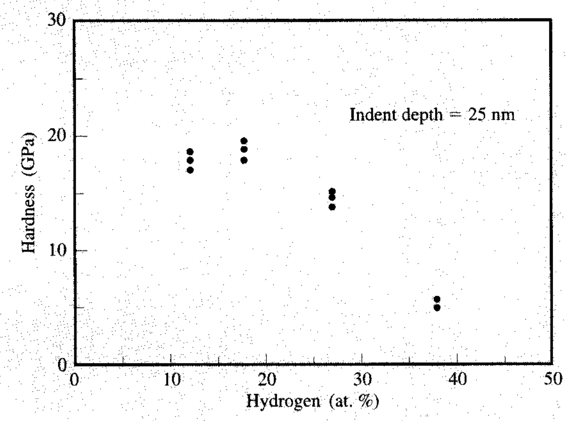

Figure 18

Effects of hydrogen incorporation in carbon on its hardness.

can interfere with the flying characteristics of the slider. An additional requirement, which is becoming more important for disk files intended for laptop computer applications, is the maintenance of a low-friction interface through the life of the file. Laptop computer disk files are designed with low-power-consumption, low-torque motors.

While there are many parameters affecting the durability performance of thin-film disks (slider material and contact dynamics, disk lubricant and texture, and test environment), property control of the disk overcoat is essential to disk durability. It is widely reported that the a–C:H films provide superior performance compared to the a–C sputtered overcoats. Marchon, Heiman, and Khan [90] have attributed this improved performance to the higher degree of sp^3 bonding that is obtained for suitably hydrogenated films. They have demonstrated the strong detrimental effect of oxygen in the test environment and have cited this as evidence for a tribochemical wear mechanism. Carbon at the film surface is oxidized to CO and CO_2 and is tribochemically desorbed. The lack of disk debris found during disk wear testing in oxygen environments is further evidence that this mechanism may be operative. The presence of hydrogen promotes the formation of the more oxidation-resistant sp^3-bonded carbon and terminates dangling bonds in the carbon structure, which may make it less prone to oxidative degradation.

Improved tribochemical performance may not be the only mechanism operating which improves the a–C:H performance. Other studies have reported that improved interaction of the a–C:H with the topical lubricant improves disk durability [91]. In addition, tribochamber studies in nonoxidizing UHV environments find that durability performance improves with overcoat hydrogenation.[1] Agarwal, Li, and Heiman [92] recently found evidence that this oxidative wear mechanism may be primarily applicable to the a–C films and that abrasive/adhesive wear may be more important for the a–C:H films. For abrasive/adhesive wear, improved hardness is key to improving wear resistance. Other studies have demonstrated that improved wear-in friction performance can be obtained with increased hardness in a–C films [86].

- *Future directions*

An important issue for thin-film disk manufacturing is defect generation. Carbon targets are known to produce film defects by ejecting small graphite particles which can become embedded in the disk [93]. For sputtering processes which generate resistive films, the potential for target arcing is present, which generates particles within the sputter system. As data storage densities increase, sliders will be required to fly even closer to the disk surface ($\leq$50 nm). In addition, as bit cell sizes decrease, the issue of magnetic defects will assume increasing importance. For both these reasons, deposition processes for future overcoats will be pushed to become defect-free.

Closely related to sputter defects are the magnetic defects associated with irregularities in the underlying Ni–P texture. For advanced media, sufficiently low data error rates require that the Ni–P texture become smoother. Traditionally, the roughness of the texture has been used to reduce the slider-to-disk contact area and thus the friction forces. One alternative is to put the texture in the overcoat rather than under the magnetic layer. A glass-substrate-based disk is commercially available which possesses such an overcoat [62]. It is, however, not a sputtered overcoat and is therefore not compatible with the considerable capital investment the industry has in large-scale sputter deposition tooling.

The industry standard overcoat thickness is in the 150–200-Å range. Modeling for the 10-Gb/in.^{2} disk storage density suggests that overcoat thickness must be reduced to $\approx$50 Å in order to achieve the magnetic spacing required for these high densities. To achieve reliable performance with films this thin, significant evolution in the properties of the texture, lubricant, and overcoat will be required. In fact, for goals this aggressive, it is not clear that evolution alone will be sufficient. Invention of new materials or processes may be required in one or all three of the primary parameters affecting disk durability (texture, lubricant, and disk overcoat).

[1] X. Pan and R. L. White, unpublished results.

Lubrication—Materials and processes

• *General*

Lubricant is the final layer in the hierarchy of a finished thin-film disk, as shown in Figure 1. Its primary function is very similar to that of the overcoat, which is to protect the disk from friction and wear [94]. It brings additional stability to the head–disk interface by providing the recording heads with a smooth transition from a region of dragging to flying and by absorbing some of the energy that is generated by intermittent contact between head and disk during flying.

In order to qualify as a disk lubricant, a material must satisfy a number of requirements. Physical properties include chemical inertness, low vapor pressure, low surface tension, high thermal stability, stability under high shear stress, and good boundary lubrication properties [95]. It is equally important that the lubricant should reside on the disk surface over the lifetime of a product without being subjected to desorption, spin-off, and thermal degradation. Ensuring these properties has become increasingly difficult with the advent of very smooth thin-film disks.

Unlike particulate media, which were formulated to generate pores to retain and to replenish the depleted surface lubricant [96, 97], thin-film disks are made to be very smooth and free of pores. Thus, lubricant adhesion to the overcoat surface has become one of the important issues with respect to the long-term durability of thin-film disks. Adhesion is strongly influenced by the nature of the functional groups on the lubricant molecule and the functional groups on the surface of the overcoat.

• *Materials*

Since the early development of recording media, there has been a continuous search to find an optimum lubricant for disk applications. Several classes of liquid lubricants may satisfy most of the requirements mentioned above. These include the silicones, the long-chain hydrocarbons, the phosphazines, and the halocarbons. Dimethylsilicone was selected for use on the very early IBM RAMAC™ disks, primarily because of its high thermal stability and low volatility, and the lack of availability of other more suitable materials [98]. However, as the head–disk interface spacing became much smaller and as the drive operation was shifted to depend on repeated CSS cycles, silicones were found to be unacceptable because of their poor boundary lubrication properties [99]. Although some of the long-chain liquid hydrocarbons such as squalane and tridecylstearate were found to have excellent lubrication properties,[2] they were not chosen because of their high volatility and high surface tension and the potential of tribopolymer formation [100]. On the other hand, some of the long-chain solid hydrocarbons, such as fatty acids, have been successfully used as disk lubricants, assuming that a replenishment mechanism can be provided within the disk drive [101, 102]. Phosphazene lubricants, such as X1P made by Dow Chemical [103], have also shown promise for lubricating disks under high stress conditions, i.e., high temperatures and humidities [104]. These lubricants were originally developed for aircraft gas turbine engines and have extremely low vapor pressure, high thermal stability, and good solubility in non-CFC solvents (i.e., more environmentally safe solvents) [105].

Among the many halocarbons that are available today, liquid perfluoropolyethers (PFPEs) stand out as the most suitable lubricant for disk applications [104, 106]. Their molecular composition consists essentially of carbon, oxygen, and fluorine atoms, which provide the required chemical and thermal stability as well as the molecular flexibility demanded for lubrication. Their superiority as disk lubricants derives mostly from their wide range of fluidity, great lubricity, low surface tension, and excellent thermal and chemical stability [107]. Three main classes of PFPEs are commercially available: KRYTOX®, Fomblin® Y, Fomblin Z, and Demnum® [108]:

$$\mathrm{F{-}(}\underset{\displaystyle \mathrm{CF_3}}{\underset{|}{\mathrm{CF}}}\mathrm{{-}CF_2{-}O{-})}m\mathrm{{-}CF_2{-}CF_3}$$

KRYTOX

$$\mathrm{CF_3{-}O{-}(}\underset{\displaystyle \mathrm{CF_3}}{\underset{|}{\mathrm{CF}}}\mathrm{{-}CF_2{-}O{-})}m\mathrm{{-}(CF_2{-}O{-})}n\mathrm{{-}CF_3}$$

Fomblin Y: $m/n > 40$

$$\mathrm{CF_3{-}O{-}(CF_2{-}CF_2{-}O{-})}p\mathrm{{-}(CF_2{-}O{-})}q\mathrm{{-}CF_2{-}OH}$$

Fomblin Z: $p/q < 1$

$$\mathrm{F{-}(CF_2{-}CF_2{-}CF_2{-}O{-})}m\mathrm{{-}CF_2{-}CF_3}$$

Demnum

KRYTOX and Fomblin Y are branched polymers which were used primarily on particulate disks for IBM 3380 and 3390 drives. Fomblin Z and Demnum are linear polymers and have been investigated mostly for thin-film disks. Although the long-chain Fomblin Z fluids (molecules without functional end-groups) have been found to have better lubrication properties than the KRYTOX and Fomblin Y [109], they are also known to be thermally less stable because of their increased number of carbon–oxygen bonds (see **Figure 19**). Nevertheless, the Fomblin Z fluids are the most common lubricants in use. Although Demnums are known to be more stable, they are relatively new, and their potential is still under evaluation.

[2] A. W. Wu and M. Parker, unpublished results.

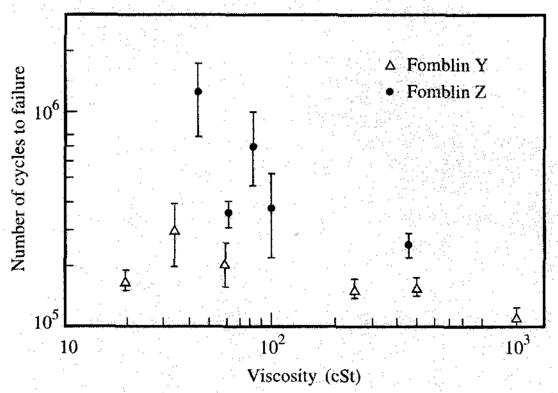

Figure 19

Wear performance of Fomblin-lubricated disks.

Another key factor in lubricant design is the affinity of the reactive or polar end-group to the overcoat surface. This affinity greatly enhances the lubricants' resistance to being squeezed out from between two contacting surfaces [110]. This resistance allows for hydrodynamic and boundary lubrication to be maintained at a much higher load and reduces the probability of damaging solid–solid adhesion and shearing. To enhance the adhesion of PFPE lubricants to the carbon surfaces of the disk, a series of bifunctionally terminated PFPE polymers such as Fomblin ZDOL with hydroxy end-groups and Fomblin AM2001 with piperonyl end-groups are now available [111–113]:

$HO–CH_2–CF_2–(CF_2–CF_2–O–)p–$
$(CF_2–O–)q–CF_2–CH_2–OH$

Fomblin ZDOL

$P–CH_2–O–CH_2–CF_2–(CF_2–CF_2–O–)p–$
$(CF_2–O–)q–CF_2–CH_2–O–CH_2–P$

Fomblin AM2001

P = piperonyl group

The selection of ZDOL or AM2001 for disk applications depends heavily on the type of overcoat that is used. For a SiO_2 overcoat, ZDOL is generally preferred [114, 115], whereas for carbon overcoats, both ZDOL and AM2001 are more frequently employed [116].

- *Lubricant–surface interface*

In general, studies have shown that the perfluoropolyether polymer backbone interacts with surfaces mainly via van der Waals interactions [117–119]. Takeuchi et al. have observed an increase in the van der Waals bonding energy of 6 kJ/mol for each CF_2 unit added to the polymer backbone [118]. Similar backbone bonding energies are observed for perfluoropolyethers on the surfaces of carbon films [119]. The van der Waals interaction with the disk surface is sufficiently strong to ensure that the molecules lie flat on the surface when the lubricant film thickness is comparable to the 7-Å polymer chain diameter [117]. If the film thickness is increased above a chain diameter, the van der Waals interactions with the disk decrease rapidly [117]. Consequently, for a slider sitting on disks with thicker liquid lubricant films, the capillary pressure of lubricant that has formed menisci around the contacting asperities can pull more lubricant into the slider–disk interface, which results in increasing stiction forces with increasing liquid lubricant film thickness [120]. The addition of functional end-groups, of course, strengthens the interaction of the lubricant molecules with the disk surface, decreasing stiction effects.

The improved adhesion of AM2001 and ZDOL to overcoat surfaces is thought to come from the molecular interactions between the end-groups and the overcoat surface. It has been proposed that the molecular interactions occur through hydrogen bonding for ZDOL [121] and through π–π-bond interaction for the AM2001 [116] (**Figure 20**). However, the existence of these physical or chemical interactions is difficult to prove. Suggestive data are derived from indirect analyses such as X-ray reflectivity [122], ESCA [123–125], FTIR [116, 126], and molecular engineering studies [127, 128].

To further promote the adhesion between the polar end-group-terminated PFPE and the overcoat surfaces, various treatment methods have been explored, including those of heat [129], UV [130, 131], and plasma.[3] Among these techniques, only heat treatment has been widely used by disk manufacturers because it is the simplest method to implement in a production environment. Again, the mechanisms for adhesion improvement are not fully understood. There is only indirect experimental evidence to suggest some preferred orientation of the lubricant molecules after the heat treatment. Some of the strongest evidence comes from the water contact-angle measurements on a lubricated disk surface before and after heat treatment. There is a gradual increase in the water contact angle as the temperature rises.[4] The result is shown in **Figure 21**. This suggests that the fluorine atoms of the lubricant molecules preferentially orient themselves toward the air of the air–disk interfaces, with the oxygen atoms and polar end-groups anchoring more strongly to the lubricant–overcoat interfaces. It has been proposed

[3] J. Lin, D. Saperstein, and A. H. Homola, unpublished results.
[4] W. T. Tang, unpublished results.

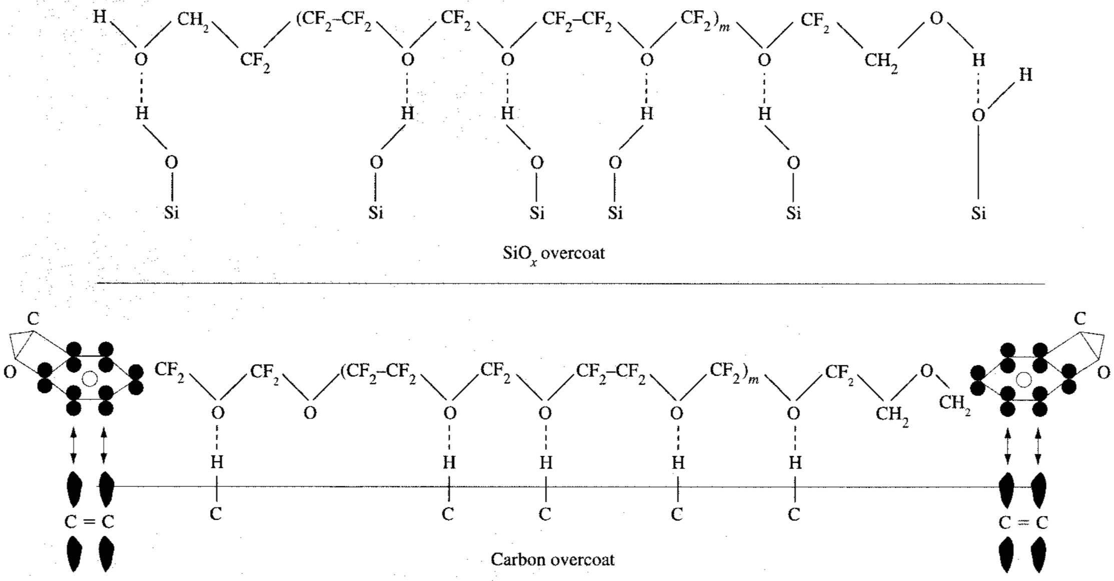

Figure 20

Comparison of SiO_2 and carbon-overcoated media.

that the heat treatment is necessary to provide a cleaner interface for the lubricant to interact more intimately by driving off the absorbed water molecules and other contaminants, and also to provide the necessary activation energy for the lubricant molecules to orient and to react. A simple method often used to distinguish the anchored (bonded) lubricant from that of the free fraction on the disk surfaces is by an extraction with freon or other fluorinated solvents. The free lubricant is readily removed, whereas the bonded fraction remains on the surfaces. A subsequent water contact angle or FTIR measurement confirms the presence of the bonded lubricant.

The use of only bonded lubricant on the disk surface is not sufficient to protect the disks from many CSS cycles, since there is no replenishment mechanism available to replace what has been removed from the worn area. A sufficient quantity of the free lubricant is needed to ensure long-term durability of the disks [132]. However, the balance between the amount of free and bonded lubricant must be very carefully controlled. The presence of any excessive amount of free lubricant on the disk surfaces will increase stiction (static friction), which is defined as the amount of tangential force required for a slider to break away from a disk surface after resting [133–138]. As the disk surfaces become smoother to accommodate higher areal densities, the occurrence of stiction is more likely, since most of the lubricant now resides on the head–disk interface.

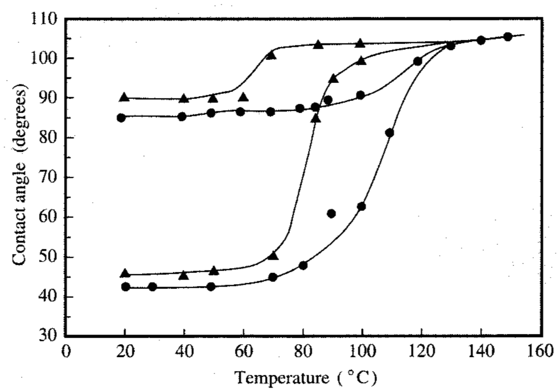

Figure 21

Contact-angle performance of several lubricants.

Another element that can further complicate the stiction problem is the interaction among the overcoat, the lubricant, and the water molecules. A strong correlation has been established between relative humidity and stiction values [139–146]; the effect is especially pronounced for humidity exceeding 80%. Even on the very hydrophobic surfaces of a disk lubricated with perfluoropolyether, at high humidities some water condenses amongst the lubricant molecules and can even unbond some of the bonded species [147, 148]. While adsorbed water usually enhances the durability of contacting surfaces, it raises the stiction forces of the slider–disk interface because water menisci which have high surface tension forces at the contacting asperities must be sheared. The use of bonded lubricant alleviates some of the stiction problems [149], but incurs the risk of long-term durability failure. It should be pointed out that there are other additional factors which can also contribute to the stiction problem, including slider load, slider design, length of storage, and the interaction between the lubricant and the contaminants often found in the drives [150].

- *Lubrication processes*

A number of manufacturing processes are available for depositing a lubricant onto the disk surface, including dipping and draining, spraying, and spin-coating. To achieve a better lubricant uniformity across the disk surface, wiping is often included as a final part of the process. Because of its simplicity and high throughput, dipping and draining has become the method preferred by most disk manufacturers. The lubricant thickness for thin-film disks is generally very thin, usually 5–25 Å. In the dipping process, the lubricant thicknesses are controlled by the disk withdrawal speed and the lubricant concentration in a fluorinated solvent. Similarly, in the draining process, the lubricant thicknesses are controlled by the drain rate and the lubricant concentration. Since ambient conditions such as temperature and humidity can affect the final thickness, they must be under tight control.

Another important element in the lubrication process is the measurement of lubricant thickness. The techniques that are commonly used today include Fourier-transform infrared spectroscopy (FTIR) [151–154], electron spectroscopy for chemical analysis (ESCA) [155–161], secondary ion mass spectroscopy (SIMS) [162], and ellipsometry [163–165]. There are good correlations among all of the measuring tools. They are, in fact, often used concurrently as a means to cross-check thickness. One of the primary weaknesses of these techniques is their area of sampling—usually a few mm in diameter. Extrapolation of these values to the average lubricant thickness of a full disk can be difficult and also involves tedious measurements. Techniques which can be used to measure the lubricant distribution over a larger area, such as the radioactive assaying of the lubricant followed by the measurement of fluorescence intensity [166, 167], are not sensitive enough to be used when the lubricant thickness approaches the molecular level. On the other end of the spectrum, analytical techniques that can determine the lubricant thickness and uniformity on a microscopic level include scanning tunneling microscopy (STM) [168] and atomic force microscopy (AFM) [169].

Within a disk drive, the disks rotate at several thousand RPM. When under such a high centrifugal force, a liquid lubricant has the tendency to migrate from ID to OD and eventually spin off from the disk surface [170–177]. Unfortunately, there is a trade-off between lubricant spin-off and durability. The lubricant must be mobile enough to quickly replenish lubricant removed during head–disk contacts, but not so mobile that it easily spins off the disk. Lubricant can be moved from one part of the disk to another in a number of ways:

1. The lubricant can be moved by means of surface forces such as van der Waals interactions with the disk surface or the affinity of the end-groups [110].
2. Centrifugal forces can cause lubricant to slowly spin off the disk.
3. Evaporation of the lubricant from one part of the disk can be followed by redeposition on other parts of the disk or elsewhere in the disk drive [178, 179].
4. The slider can pick up lubricant during contact with one part of the disk and redeposit it on another part of the disk.

Consequently, to minimize spin-off and maximize durability, one should use lubricants with very low vapor pressures and high affinities to the disk surface. However, liquids that have low vapor pressure tend to have high viscosities and consequently poor mobilities and poor durabilities (Figure 19). It also helps to use low RPM and high flying heights to minimize spin-off and slider transport of lubricant; however, to achieve higher performance in future files, it will be necessary to spin faster and fly lower than is currently being done today.

- *Future trends*

If liquid lubricants are to be used on advanced future thin-film disks, it is important that a fundamental understanding of the lubrication mechanism be obtained. This includes lubricant dynamics under sliding and flying conditions, lubricant structure and its conformation on the surface, lubricant displacement by the contaminants often found in a drive environment, the true bonding mechanism of the bonded lubricant, lubricant decomposition under long-term exposure to high shear stresses, the implications of degraded lubricant on disk durability, and finally, the importance of the triboelectrical effect on lubricant decomposition. As head–disk interface technology approaches that of contact or near-contact recording, an era of molecular tribology, it becomes increasingly urgent to find a lubricant that will endure continuous dragging of the slider on a very smooth disk surface at high speed without suffering spin-off, friction-induced decomposition, or lubrication-contamination interference.

For advanced future thin-film disks, it may be necessary to discard the traditional approach of using a liquid lubricant. Research effort should be devoted to evaluating solid lubricants which may alleviate some of the classic problems, most notably wear and debris accumulation. There are already reports which address the potential application of some of the solid lubricants to disk technology [180–181]. For reasons of cost reduction, vacuum processes may also be used for lubricant deposition.

Acknowledgments

The authors wish to acknowledge the written contribution of P. Baumgart, D. Krajnovich, T. Nguyen, and A. Tam of IBM on laser texture technology. Also, we thank B. Street for his careful reading and helpful suggestions on the readability and clarity of the text.

MYLAR and KRYTOX are registered trademarks of E. I. du Pont de Nemours and Co.

RAMAC is a trademark of International Business Machines Corporation.

Fomblin is a registered trademark of Ausimont, S.p.A.

Demnum is a registered trademark of Daikin Kogyo Co., Ltd.

References

1. S. Doss and T. Michaelson, "Electroless Plating of Some Ni–P–Cu Alloys and Their Microhardness," presented at the Third Electroless Nickel Conference, Chicago, March 29–31, 1983.
2. J. K. Lee, A. Chao, J. Enguero, M. Smallen, H. J. Lee, and P. Dion, "Effect of Disk Cross Hatch Texture on Tribological Performance," *IEEE Trans. Magn.* **28**, 2880 (1992).
3. B. Bhushan, "Magnetic Slider/Rigid Disk Substrate Materials and Disk Texturing Techniques—Status and Future Outlook," *ASME Adv. Info. Stor. Syst.* **5**, 175 (1993).
4. W. C. Leung, A. Juliana, V. T. Pan, and H. J. Rosen, "Method and Apparatus for Optically Measuring Characteristics of a Thin Film by Directing a P-Polarized Beam Through an Integrating Sphere at the Brewster's Angle of the Film," U.S. Patent 4,873,430, 1990.
5. S. Hosaka, "STM/AFM/MFM Characterization of Electronic and Magnetic Materials and Their Applications," *IEEE Trans. J. Magn. in Japan* **8**, 226 (1993).
6. D. Rugar, H. J. Mamin, P. Guethner, S. E. Lambert, J. E. Stern, I. McFadyen, and T. Yogi, "Magnetic Force Microscopy: General Principles and Applications to Longitudinal Recording Media," *J. Appl. Phys.* **68**, 1169 (1990).
7. G. Binnig and H. Rohrer, "Scanning Tunneling Microscopy," *IBM J. Res. Develop.* **30**, 355 (1986).
8. Y. Martin, D. Rugar, and H. K. Wickramasinghe, "High Resolution Magnetic Images of Domains in TbFe by Force Microscopy," *Appl. Phys. Lett.* **52**, 244 (1988).
9. R. Ranjan, D. N. Lambeth, M. Tromel, P. Goglia, and Y. Li, "Laser Texturing for Low Flying Height Media," *J. Appl. Phys.* **69**, 5745 (1991).
10. P. Baumgart, D. Krajnovich, T. Nguyen, and A. Tam, "A New Laser Texturing Technique for High Performance Magnetic Disk Drives," *IEEE Trans. Magn.* **31**, Pt. 1 (Proceedings of Intermag 1995), 2946 (1995).
11. I. Molyneux, "Glass—The Substrate for Optical and Rigid Magnetic Storage Discs," presented at the IEEE Colloquium on New Materials for Information Storage, 1991.
12. K. Matsumo, K. Shukuri, T. Nakazumi, and K. Sono, "Mechanical Strength of Chemically Strengthened Glass Substrates for Disk Drives," *J. Magn. Soc. Jpn.* **13**, Suppl. No. S1, 763 (1989).
13. P. M. Ramsey, "Permaglide: Controlled Glass Surfaces," presented at the International Disk Drive Equipment and Materials Association (IDEMA) 2nd Symposium on Alternate Substrates, San Jose, CA, September 28, 1993.
14. T. Matsudaira, K. Ishizaki, and C. Krishnan, "Effects of Disk Microtexture on Glide and Modulation at Ultra-Low Flying Heights," *IEEE Trans. Magn.* **26**, Pt. 1 (Proceedings of Intermag 1990), 2429 (1990).
15. K. Ishribashi, "Texturing of Glass Disks by Microgrid Method," *J. Magn. Soc. Jpn.* **16**, 78 (1992).
16. B. Bhushan, "Magnetic Slider/Rigid Disk Substrate Materials and Disk Texturing Techniques—'Slick as Ice and Tough as Nails—The New Tribolayers,' Status and Future Outlook," *ASME Adv. Info. Stor. Syst.* **5**, 175 (1993).
17. H.-C. Tsai, "Advantage and Challenge of Nonmetallic Substrate for Rigid Disk Applications," *IEEE Trans. Magn.* **29**, 241 (1993).
18. S. Yamamoto, H. Muraoka, and Y. Nakamura, "High Areal Bit Density Perpendicular Magnetic Recording on Hard Disk," *IEEE Trans. Magn.* **27**, 5292 (1991).
19. K. Hara, T. Kogure, S. Katayama, and S. Furusawa, "Recording Performance of CoNiCr Rigid Disks Using Glass Substrates," *IEEE Trans. Magn.* **27**, 5028 (1991).
20. T. Kogure, S. Katayama, and N. Ishii, "High Coercivity Magnetic Hard Disks Using Glass Substrates," *J. Appl. Phys.* **67**, 4701 (1990).
21. D. J. Mapps, G. Parr, M. A. Akhter, S. Onodera, and A. Okabe, "In-Contact Magnetic Recording Performance of Pt/CoCrTa Thin-Films on Glass Computer Disks," *J. Magn. & Magnet. Mater.* **120**, 305 (1993).
22. T. Li, E. Rabinowicz, and N. Saka, "Friction Characteristics and Wear Resistance of Carbon-Coated Glass-Based Rigid Magnetic Disks," *Wear* **143**, 241 (1991).
23. T. Matsudaira and C. S. Krishnan, *Hoya Electronic Company Newsletter*, No. 6 (October 1991); available from the Hoya Corporation, Akishima, Tokyo, Japan.
24. G. L. Chan, J. Shir, and T. Chen, "High Coercivity, Low Noise and Low Bit Shift on Sputtered Thin-Film Glass Disks," presented at the 4th Joint MMM-Intermag Conference, Vancouver, Canada, July 12–15, 1988.
25. H.-C. Tsai and A. Eltoukhy, "Head Flying Characteristics on Canasite Disks," *IEEE Trans. Magn.* **27**, 5140 (1990).
26. J. Weiss, "Canasite—Rewriting Rules for Mechanical Performance," presented at the Diskcon Technical Conference (IDEMA), San Jose, CA, 1990.
27. D. Perettie, D. C. Burdeaux, M. McCulloch, D. E. Speliotis, R. Keinsteatd, and J. Judy, "Use of High Performance Resins for the Planarization of Magnetic Rigid Disk Substrates," *IEEE Trans. Magn.* **27**, 5175 (1991).

28. M. Kuwabara, M. Sato, Y. Ohnishi, M. R. Visokay, H. Hayashi, H. Inoue, and K. Muramatsu, "Co Alloy Media Made on Amorphous Carbon Substrate," *J. Appl. Phys.* **73**, 6686 (1993).
29. M. Sato, Y. Ohnishi, and A. Nakaue, "CoNiCr/Cr Media Prepared on Amorphous Carbon Substrate," *Proceedings of the 52nd Fall Meeting, Jpn. Soc. Appl. Phys.* **54**, 159 (1991).
30. M. Mirzamaani, C. Jahnes, and M. Russak, "Thin-Film Disks with Transient Metal Underlayers," *IEEE Trans. Magn.* **28**, 3090 (1992).
31. M. L. Williams and R. L. Comstock, "An Analytical Model of the Write Process in Digital Magnetic Recording," *AIP Conf. Proc.*, 1971, p. 738.
32. B. K. Middleton, "The Recording and Reproducing Process," *Magnetic Recording Volume I: Technology*, C. D. Mee and E. D. Daniels, Eds., McGraw-Hill Book Co., Inc., New York, 1987, p. 22.
33. E. M. T. Velu and D. N. Lambeth, "High Density Recording on SmCo/Cr Thin-Film Media," *IEEE Trans. Magn.* **28**, 3249 (1992).
34. R. A. Baugh, E. S. Murdock, and B. R. Natarajan, "Measurement of Noise in Magnetic Media," *IEEE Trans. Magn.* **MAG-19**, 1722 (1983).
35. J. A. Thornton, "The Microstructure of Sputter-Deposited Coatings," *J. Vac. Sci. Technol. A* **4**, 3059 (1986).
36. T. Yogi, T. A. Nguyen, S. E. Lambert, G. L. Gorman, and G. Castillo, "Role of Atomic Mobility in the Transition Noise of Longitudinal Media," *IEEE Trans. Magn.* **26**, 1578 (1990).
37. T. Yogi, G. L. Gorman, C. H. Hwang, M. A. Kakalec, and S. E. Lambert, "Dependence of Magnetics, Microstructures, and Recording Properties on Underlayer Thickness in CoNiCr/Cr Media," *IEEE Trans. Magn.* **24**, 2727 (1988).
38. B. R. Natarajan and E. S. Murdock, "Magnetic and Recording Properties of Sputtered Co-P/Cr Thin-Film Media," *IEEE Trans. Magn.* **24**, 2724 (1988).
39. J. N. Chapman, I. R. McFadyen, and J. P. C. Bernards, "Investigation of Cr Segregation Within RF-Sputtered CoCr Films," *J. Magn. & Magnet. Mater.* **62**, 359 (1986).
40. D. J. Rogers, J. N. Chapman, J. P. C. Bernards, and S. B. Luitjens, "Determination of Local Composition in CoCr Films Deposited at Different Substrate Temperatures," *IEEE Trans. Magn.* **25**, 4180 (1989).
41. M. R. Kim, S. Guruswamy, and K. E. Johnson, "Experimental Observation of Solute Segregation in Longitudinal CoPtCr/Cr Magnetic Thin-Films," *IEEE Trans. Magn.* **29**, 3673 (1993).
42. Y. Maeda and M. Asahi, "Segregated Microstructure in Sputtered CoCr Film Revealed by Selective Wet Etching," *J. Appl. Phys.* **61**, 1972 (1987).
43. T. P. Nolan and R. Sinclair, "Effect of Microstructural Features on Media Noise in Longitudinal Recording Media," *J. Appl. Phys.* **73**, 5566 (1993).
44. P. V. Mitchell, A. Layadi, N. S. VanderVen, and J. O. Artman, "Direct Observation of Magnetically Distinct Regions in CoCr Perpendicular Recording Media Using Ferromagnetic Resonance," *J. Appl. Phys.* **57**, 3976 (1985).
45. F. T. Parker, "Mossbauer Effect of Dilute Fe in Sputtered CoCr Films," *J. Appl. Phys.* **60**, 2498 (1986).
46. A. Murayama, M. Miyamura, S. Ishikawa, and Y. Oka, "Brillouin Study of Spin Waves in Sputtered CoNiPt Alloy Films," *J. Appl. Phys.* **67**, 410 (1990).
47. Y. Maeda and M. Takahashi, "Thermomagnetic Analysis of Compositional Separation in Sputtered CoCr Films," *J. Appl. Phys.* **68**, 4751 (1990).
48. M. Doerner, T. Yogi, T. Nguyen, D. Parker, B. Hermsmeier, and O. Allegranza, "Composition Effects in High Density CoPtCr Media," *IEEE Trans. Magn.* **29**, 3667 (1993).
49. D. J. Sellmyer, D. Wang, and J. A. Christner, "Magnetic and Structural Properties of CoCrTa Films and Multilayers with Cr," *J. Appl. Phys.* **67**, 4710 (1990).
50. K. E. Johnson, "Thin-Film Recording Media: Challenges for Physics and Magnetism in the 1990s," *J. Appl. Phys.* **69**, 4932 (1991).
51. C. R. Paik, I. Suzuki, N. Tani, M. Ishidawa, T. Ota, and K. Nakamura, "Magnetic Properties and Noise Characteristics of High Coercivity CoCrPtB/Cr Media," *IEEE Trans. Magn.* **28**, 3084 (1992).
52. E. E. Murdock, B. R. Natarajan, and R. G. Walmsley, "Noise Properties of Multilayered Co-Alloy Magnetic Recording Media," *IEEE Trans. Magn.* **26**, 2700 (1990).
53. T. Yogi, C. Tsang, T. A. Nguyen, K. Ju, G. L. Gorman, and G. Castillo, "Longitudinal Media for 1 Gb/in.^{2} Areal Density," *IEEE Trans. Magn.* **26**, 2271 (1990).
54. M. Futamoto, F. Kugiya, M. Suzuki, H. Takano, Y. Matsuda, N. Inaba, Y. Miyamura, K. Akagi, T. Nakao, H. Sawaguchi, H. Fukuoka, T. Munemoto, and T. Takagaki, "Investigation of 2 Gb/in.^{2} Magnetic Recording at a Track Density of 17kTPI," *IEEE Trans. Magn.* **27**, 5280 (1991).
55. E. Murdock, "Roadmap for 10 Gbit/in.^{2} Media: Challenges," *IEEE Trans. Magn.* **28**, 3078 (1992).
56. T. Min and J. G. Zhu, "Bicrystal Advanced Thin-Film Media for High Density Recording," *J. Appl. Phys.* **75**, 6129 (1994).
57. M. Mirzamaani, C. V. Jahnes, and M. A. Russak, "Magnetic Properties of CoCrPt Thin Films with ⟨1120⟩ Crystal Orientation," *J. Appl. Phys.* **69**, 5169 (1991).
58. J. Ding and J. G. Zhu, "Microstructure and Recording Properties of Bicrystal Disks with GaAs Substrates," *IEEE Trans. Magn.* **30**, 3978 (1994).
59. P. L. Lu and S. H. Charap, "Thermal Instability at 10 Gbit.in.^{2} Magnetic Recording," *IEEE Trans. Magn.* **30**, 4230 (1994).
60. V. Raman, "Microstructure and Mechanical Behavior of Al–Mg/Ni–P Composites," *J. Mater. Res.* **5**, 1684 (1990).
61. T. Yamashita, G. L. Chen, J. Shir, and T. Chen, "Sputtered Zirconia Overcoat with Superior Corrosion Protection and Mechanical Performance in Thin-Film Rigid Disk Application," *IEEE Trans. Magn.* **24**, 2629 (1988).
62. H. Kawai and A. Kurikawa, "Magnetic Recording Medium Capable of Recording Information at a High Recording Density," U.S. Patent 5,029,317, 1991.
63. S. Aisenberg and R. Chabot, "Ion-Beam Deposition of Thin-Films of Diamondlike Carbon," *J. Appl. Phys.* **42**, 2953 (1971).
64. F. K. King, "Datapoint Thin Film Media," *IEEE Trans. Magn.* **17**, 1376 (1981).
65. H. C. Tsai and D. B. Bogy, "Characterization of Diamondlike Carbon Films and Their Application as Over-Coats on Thin-Film Media for Magnetic Recording," *J. Vac. Sci. Technol.* **6**, 3287 (1987).
66. J. Robertson, "Hard Amorphous (Diamondlike) Carbons," *Prog. Solid State Chem.* **21**, 199 (1991).
67. J. C. Angus, W. Wang, and M. Sunkara, "Metastable Growth of Diamond and Diamondlike Phases," *Ann. Rev. Mater. Sci.* **21**, 221 (1991).
68. J. K. Howard, "Process for Making a Thin Film Metal Alloy Magnetic Recording Disk with a Hydrogenated Carbon Overcoat," U.S. Patent 4,778,582, 1988.
69. J. Zelez, "Low-Stress Diamondlike Carbon Films," *J. Vac. Sci. Technol.* **1**, 305 (1983).

70. L. Holland and S. M. Ojha, "The Growth of Carbon Films with Random Atomic Structure from Ion Impact Damage in a Hydrocarbon Plasma," *Thin Solid Films* **58**, 107 (1979).
71. J. Kaufman, S. Metin, and D. Saperstein, "Symmetry Breaking in Nitrogen-Doped Amorphous Carbon: Infrared Observation of the Raman-Active G and D Bands," *Phys. Rev. B* **39**, 13053 (1989).
72. A. Grill, B. S. Meyerson, and V. V. Patel, "Diamondlike Carbon Films by rf Plasma-Assisted Chemical Vapor Deposition from Acetylene," *IBM J. Res. Develop.* **34**, 849 (1990).
73. J. C. Angus and C. C. Hayman, "Low-Pressure, Metastable Growth of Diamond and Diamondlike Phases," *Science* **241**, 913 (1988).
74. H. C. Tsai, D. B. Bogy, M. K. Kundmann, D. K. Veirs, M. R. Hilton, and S. T. Mayer, "Structure and Properties of Sputtered Carbon Overcoats on Rigid Magnetic Media Disks," *J. Vac. Sci. Technol.* **16**, 2307 (1988).
75. B. Marchon, M. Salmeron, and W. Siekhaus, "Observation of Graphitic and Amorphous Structures on the Surface of Hard Carbon Films by Scanning Tunneling Microscopy," *Phys. Rev. B* **39**, 12907 (1989).
76. F. Jansen, M. A. Machonkin, S. Kaplan, and S. Hark, "The Effects of Hydrogenation on the Properties of Ion Beam Sputter Deposited Amorphous Carbon," *J. Vac. Sci. Technol.* **3**, 605 (1985).
77. D. Beeman, R. Lunds, and M. R. Anderson, "Modeling Studies of Amorphous Carbon," *Phys. Rev. B* **30**, 870 (1984).
78. A. Richter, H. J. Scheibe, W. Pompe, K. W. Brzezinka, and I. Muehling, "About the Structure and Bonding of Laser Generated Carbon Films by Raman and Electron Energy Loss Spectroscopy," *J. Non-Cryst. Solids* **88**, 131 (1984).
79. M. A. Tamor, J. A. Haire, C. H. Wu, and K. C. Hass, "Correlation of the Optical Gaps and Raman Spectra of Hydrogenated Amorphous Carbon Films," *Appl. Phys. Lett.* **54**, 123 (1989).
80. G. Galli, R. M. Martin, R. Car, and M. Parrinello, "Structural and Electronic Properties of Amorphous Carbon," *Phys. Rev. Lett.* **62**, 555 (1989).
81. M. A. Tamor, W. C. Vassell, and K. R. Carduner, "Atomic Constraint in Hydrogenated 'Diamondlike' Carbon," *Appl. Phys. Lett.* **58**, 592 (1991).
82. J. K. Lee, M. Smallen, J. Enguero, H. J. Lee, and A. Chao, "The Effect of Chemical and Surface Properties of Hydrogenated Carbon Overcoats on the Tribological Performance of Rigid Magnetic Disks," *IEEE Trans. Magn.* **29**, 276 (1993).
83. N. F. Mott and E. A. Davis, *Electronic Processes in Non-Crystalline Materials*, 2nd ed., Clarendon Press, Oxford, England, 1979, p. 289.
84. E. Rabinowicz, *Friction and Wear of Materials*, John Wiley & Sons, Inc., New York, 1965, p. 168.
85. N. Savvides and B. Window, "Diamondlike Amorphous Carbon Films Prepared by Magnetron Sputtering of Graphite," *J. Vac. Sci. Technol.* **3**, 2386 (1985).
86. R. L. White, M. F. Doerner, and G. W. Walker, "Mechanical Properties of Carbon Films for Thin-Film Disks," *Mater. Res. Soc. Symp. Proc.* **188**, 213 (1990).
87. G. Gille and B. Rau, "Buckling Instability and Adhesion of Carbon Layers," *Thin Solid Films* **120**, 109 (1984).
88. A. Grill and V. Patel, "Stresses in Diamondlike Carbon Films," *Diamond & Rel. Mater.* **2**, 1519 (1993).
89. D. Franceschini, C. Achete, F. Freire, and G. Mariotto, "Internal Stress in Nitrogen Doped Diamondlike *a-C:H* Films," *Mater. Res. Soc. Symp. Proc.* **270**, 481 (1992).
90. B. Marchon, N. Heiman, and M. R. Khan, "Evidence for Tribochemical Wear on Amorphous Carbon Thin-Films," *IEEE Trans. Magn.* **26**, 168 (1990).
91. T. Sugiyama, T. Shinohara, K. Tanaka, and A. Shimamoto, "Hydrogenated I-Carbon Properties for Thin-Film Disks," *J. Magn. Soc. Jpn.* **15**, 595 (1991).
92. S. Agarwal, E. Li, and N. Heiman, "Structure and Tribological Performance of Carbon Overlayer Films," *IEEE Trans. Magn.* **29**, 264 (1993).
93. C. W. Chen, D. M. Makowiecki, C. S. Alford, M. A. McKernan, and P. B. Ramsey, "Surface-Defect Formation in Graphite Targets During Magnetron Sputtering," *J. Vac. Sci. Technol.* **4**, 3157 (1990).
94. T. Kita, "The Influence of Lubrication on Head and Disk Wear," *Tribology Trans.* **35**, 551 (1992).
95. E. Klaus and B. Bhushan, "Lubricants in Magnetic Media—A Review," *Tribology and Mechanics of Magnetic Storage Systems* **SP-19** (STLE—Society of Tribologists and Lubrication Engineers), 7–15 (1985).
96. P. V. Bagatta, "Concepts of Advanced Lubricant System for All Forms of Magnetic Media," presented at the Symposium on Memory and Advanced Recording Technologies, San Jose, CA, 1986.
97. J. W. Coburn and H. F. Winters, "Ion-Induced Volatilization (IIV): A Method for Quantitative Measurement of the Amounts of Perfluoro-Polyether Lubricant on a Particulate Disk Surface and in the Media Porosity," *J. Appl. Phys.* **60**, 3309 (1986).
98. J. M. Harker, D. W. Brede, R. E. Pattison, G. R. Santana, and L. G. Taft, "A Quarter Century of Disk File Innovation," *IBM J. Res. Develop.* **25**, 677 (1981).
99. J. D. Cogdell, M. C. Dawson, F. F. Ling, and S. F. Murray, "Surface Texture Effects on Thin-Film Lubrication of Steel by Silicones," *STLE Trans.* **30**, 141 (1987).
100. J. L. Lauer and W. R. Jones, "Friction Polymer," *Tribology and Mechanics of Magnetic Storage Systems* **SP-21**, 14–19 (1986).
101. T. A. Gregory, C. G. Keller, B. E. Kennedy, B. E. Murray, and W. J. Rothschild, "Method and Apparatus for Lubricating a Magnetic Disk Continuously in a Recording File," U.S. Patent 4,789,913, 1988.
102. J. L. Beck, T. P. Fracek, N. F. Misso, and D. Stucky, "Disk Drive Lubricant Reservoir," U.S. Patent 5,138,506, 1992.
103. B. S. Nader, K. K. Kar, T. A. Morgan, C. E. Pawloski, and W. L. Dilling, "Development and Tribological Properties of New Cyclotriphosphanzene High Temperature Lubricants for Aircraft Gas Turbine Engines," *STLE Tribol. Trans.*, *J. Tribol.* **35**, 37 (1992).
104. M. Yang, F. E. Talke, D. J. Peretti, T. A. Morgan, and K. K. Kar, "Environmental Effects on Phosphazene Lubricated Thin-Film Disks," *IEEE Trans. Magn.* **30**, 4143 (1994).
105. T. L. Loran, "Lubricant for Magnetic Member," U.S. Patent 4,188,434, 1980.
106. D. Schaefer, H. Mortz, D. Mayer, P. Deigner, J. Hack, and T. Falk, "Rigid Magnetic Recording Disk Having Perfluoropolyether Lubricants," U.S. Patent 4,327,139, 1987.
107. D. Sianesi, B. Zamboni, R. Fontanelli, and M. Bianaghi, "Perfluoropolyethers: Their Physical Properties and Behavior at High and Low Temperatures," *Wear* **18**, 85 (1971).
108. Y. Ohsaka, "Perfluoropolyethers," *J. Jpn. Petroleum Inst.* **8**, 1 (1985).
109. A. M. Scarati and G. Caporiccio, "Frictional Behavior and Wear Resistance of Rigid Disks Lubricated with Neutral and Functional Perfluoropolyethers," *IEEE Trans. Magn.* **MAG-23**, 106 (1987).
110. C. M. Mate, "Atomic Force Microscope Study of Polymer Lubricants on Silicon Surfaces," *Phys. Rev. Lett.* **68**, 3323 (1992).
111. D. G. Pedrotty, "Rigid Magnetic Recording Disk

Lubricated with Fluorinated Telechelic Polyethers," U.S. Patent 4,268,556, 1981.
112. G. Caporiccio, "A New Series of Lubricants for Magnetic Recording Media from Bifunctional Perfluoropolyether Derivatives," *Proceedings of the Symposium on Memory and Advanced Recording Technologies*, Paper No. WS-3C-2, Magnetic Media Information Services, San Jose, CA, 1986.
113. T. Kudo and H. Ishihara, "Magnetic Recording Medium Comprising a Surface Treatment Layer Provided on the Magnetic Layer of Specified Fluorocarboxylic Acid Amine Salts," U.S. Patent 5,093,211, 1992.
114. M. Yanagisawa, "Adsorption and Configuration of Lubricant Molecules on Overcoat Materials," *Wear* **168**, 167 (1993).
115. M. Yanagisawa, "An Adsorption of Perfluoropolyethers on SiO_2 Surfaces for Thin-Film Magnetic Disk Overcoats," *ASME Tribol. Trans.* **36**, 484 (1993).
116. K. Merchant, P. Mee, M. Smallen, and S. Smith, "Lubricant Bonding and Orientation on Carbon Coated Media," *IEEE Trans. Magn.* **26**, 2688 (1990).
117. C. M. Mate and V. J. Novotny, "Molecular Conformation and Disjoining Pressure of Polymeric Liquid Films," *J. Chem. Phys.* **94**, 8420 (1991).
118. K. Takeuchi, S. S. Perry, M. Salmeron, and G. A. Somorjai, "The Bonding Properties of Hydrogenated and Fluorinated Molecules to Zirconium Oxide Thin Films: Influence of Surface Defects and Water Coadsorption," *Surf. Sci.* **323**, 30 (1995).
119. S. S. Perry, G. A. Somorjai, C. M. Mate, and R. White, "The Interaction of Short Chain Model Lubricants with the Surfaces of Hydrogenated Amorphous Carbon Films," *Tribol. Lett.* **1**, 47 (1995).
120. C. M. Mate, "Application of Disjoining and Capillary Pressure to Liquid Lubricant Films in Magnetic Recording," *J. Appl. Phys.* **72**, 3084 (1992).
121. M. Yanagisawa, "Molecular Dynamics of Thin Lubricant Films on Sol-Gel SiO_2 Surfaces for Thin-Film Magnetic Disks," *STLE Trans. Tribol.* **37**, 629 (1994).
122. M. Toney and C. Thompson, "X-Ray Reflectivity on Perfluoro-Polyether Polymer Molecules on Amorphous Carbon," *J. Chem. Phys.* **92**, 3781 (1990).
123. K. Nishimori, K. Tanaka, and Y. Inone, "Characterization of Lubricated States on Carbon Coated Media by Low Energy Photoelectron Spectroscopy Method in Ambient Atmosphere," *J. Appl. Phys.* **69**, 8042 (1991).
124. P. Herrera-Fierro, W. Jones, and S. Repper, "Interfacial Chemistry of Perfluoropolyether Lubricant Studies by X-Ray Photoelectron Spectroscopy and Temperature Desorption Spectroscopy," *J. Vac. Sci. Technol. A* **11**, 354 (1993).
125. D. Dwight, "Studies of Poly(perfluoroether). Interactions with Sputtered Carbon Overlayers on Metal Thin Film Hard Disks," Seminar at IBM, October 1990.
126. K. Johns, C. Corti, L. Montagna, and P. Srinivasan, "Development in Fluorinated Liquid Lubricants and Lubricant Additives," *J. Phys. D: Appl. Phys.* **25**, A141 (1992).
127. Y. Andoh, S. Oguchi, R. Kaneko, and T. Miyamoto, "Evaluation of Very Thin Lubricant Films," *J. Phys. D: Appl. Phys.* **25**, A71 (1992).
128. T. Tada and T. Kato, "Fluidity and Adsorption Force of Lubricants on Thin Film Magnetic Rigid Disks," *IEEE Trans. Magn.* **27**, 5172 (1991).
129. J. Ruhe, G. Blackman, V. Novotny, T. Clark, G. B. Street, and S. Kuhn, "Terminal Attachment of Perfluorinated Polymers to a Solid Surface," *Research Report RJ-9005*, IBM Research Laboratory, San Jose, CA, 1992.
130. D. Saperstein and L. Lin, "Improved Adhesion and Coverage of Perfluoropolyether Lubricant on Magnetic Disks Following Far-UV Irradiation," *Langmuir* **6**, 1522 (1990).
131. H. Tian and T. Matsudaira, "Tribological Characteristics of Liquid Lubricant on Magnetic Disks Treated by Far-UV Radiation," *Trans. ASME* **115**, 400 (1993).
132. M. Barlow, M. Braitgerg, L. Davis, V. Dunn, and D. Frew, "Duplex Reactive Fluorocarbon Film with Spin-Off Resistant Characteristics," *IEEE Trans. Magn.* **MAG-23**, 3335 (1987).
133. C. C. Liu and P. B. Mee, "Stiction at the Winchester Head–Disk Interface," *IEEE Trans. Magn.* **MAG-19**, 1659 (1983).
134. T. L. Streator, "Modeling Stiction in Liquid-Lubricated Slider–Disk Contacts," *ASME Adv. Info. Stor. Syst.* **5**, 397 (1993).
135. B. Bhushan and M. T. Dugger, "Liquid-Mediated Adhesion at the Thin Film Magnetic Disk/Slider Interface," *ASME J. Tribol.* **112**, 217 (1990).
136. A. H. Homola, "The Role of Interfacial Forces and Lubrication in Thin Film Magnetic Media," *ASME Adv. Info. Stor. Syst.* **1**, 279 (1991).
137. M. J. Matthewson and H. J. Mamin, "Liquid Mediated Adhesion of Ultra-Flat Solid Surfaces," *Mater. Res. Soc. Symp. Proc.* **19**, 87 (1988).
138. J. L. Streator, I. Etsion, and D. B. Bogy, "The Effect of Lubrication on the Static and Low-Speed Dynamic Friction in Thin Film Disks," *Tribology and Mechanics of Magnetic Storage Systems* **SP-25**, 24 (1988).
139. R. S. Timist and G. Stratford, "Effect of Humidity on Friction at Magnetic Head/Hard Disk Interfaces," *Tribology and Mechanics of Magnetic Storage Systems* **SP-25**, 17 (1988).
140. T. Miyamoto, Y. Ando, S. Hirono, and I. Sato, "Influence of Relative Humidity on Friction Characteristics of Thin Film Disk Media," *J. Magn. Soc. Jpn.* **13**, Supplement No. 51, 207 (1989).
141. Z. Li, E. Rabinowicz, and N. Saka, "The Stiction Between Magnetic Recording Heads and Thin Film Disks," *Tribology and Mechanics of Magnetic Storage Systems* **SP-26**, 64 (1988).
142. Y. Li and F. E. Talke, "A Model for the Effect of Humidity on Stiction of Head/Disk Interface," *Tribology and Mechanics of Magnetic Storage Systems* **SP-29**, 79 (1990).
143. H. Tian and T. Matsudaira, "Effect of Relative Humidity on Friction Behavior of the Head/Disk Interface," *IEEE Trans. Magn.* **28**, 2530 (1992).
144. H. Tian and T. Matsudaira, "The Role of Relative Humidity, Surface Roughness and Lubricant Migration on Static Friction Behavior of the Head/Disk Interface," presented at the ASME/STLE Tribology Conference, San Diego, CA, October 18–21, 1992.
145. Y. Li, D. Trauner, and F. E. Talke, "The Effect of Humidity on Stiction and Friction at the Head/Disk Interface," *IEEE Trans. Magn.* **26**, 2487 (1990).
146. K. Merchant and S. Smith, "Effect of Relative Humidity on Lubricant Performance," *IEEE Trans. Magn.* **29**, 3930 (1993).
147. M. Binggeli and C. M. Mate, "Influence of Capillary Condensation on Nanotribology Studied by Force Microscopy," *Appl. Phys. Lett.* **65**, 415 (1994).
148. M. Binggeli and C. M. Mate, "Influence of Water Vapor on Nanotribology Studied by Friction Force Microscopy," *J. Vac. Sci. Technol. B* **13**, 1312 (1995).
149. N. Gitis, L. Volpe, and R. Sonnenfeld, "Long Term Stiction at the Magnetic Thin Film Disk–Slider Interface," *ASME Adv. Info. Stor. Syst.* **3**, 91 (1991).
150. M. Smallen, P. Mee, K. Merchant, and S. Smith, "Contamination Induced Stiction in Drive Level Studies," *IEEE Trans. Magn.* **26**, 2505 (1990).

151. V. Au-Yeung, "FTIR Determination of Fluorocarbon Lubricant Film on Magnetic Disk Media," *IEEE Trans. Magn.* **MAG-19**, 1662 (1983).
152. Y. Kimachi, F. Yoshimura, M. Hoshino, and A. Terada, "Uniformity Quantification of Lubricant Layer on Magnetic Recording Media," *IEEE Trans. Magn.* **MAG-23**, 2392 (1987).
153. R. S. Timist, S. Ohira, and C. V. Pelow, "Tribological Properties of Boundary Lubricant Molecular Films," *Proceedings of the Japan International Tribology Conference*, Nagoya, Japan, 1990, p. 1301.
154. D. Saperstein, "IR Spectroscopy of Polyperfluoroethylene Oxide Lubricants on Amorphous Carbon," *Research Report RJ-6093*, IBM Research Laboratory, San Jose, CA, 1987.
155. B. E. Linder and P. B. Mee, "ESCA Determination of Fluorocarbon Lubricant Film Thickness on Magnetic Disk Media," *IEEE Trans. Magn.* **MAG-18**, 1073 (1982).
156. D. J. Pocker, "Angle Resolved X-Ray Photoelectron Spectroscopy Applied to Patchy Surfaces," *SPIE Proc.* **690**, 78 (1986).
157. R. Cormia, J. Smith, and L. Bernard, "Hard Disk Failure Analysis," *Solid State Technol.* **31**, 127 (1988).
158. G. T. K. Swami, "Variable Angle XPS Investigation of Lubricant Films Coated on Sputter Carbon," *Surf. & Interface Anal.* **14**, 3 (1989).
159. K. Nishimora, K. Tanaka, and S. Sato, "Evaluation of the Electron Attenuation Length for the Determination of the Lubricant Overlayer Thickness on Magnetic Disks with X-Ray Photoelectron Spectroscopy," *J. Vac. Sci. Technol. A* **8**, 3300 (1990).
160. T. Amemiya, T. Kobayashi, Y. Umeda, and Y. Nihei, "XPS Determination of Lubricant Film Thickness on Thin Film Magnetic Recording Disk," *IEEE Trans. Magn. Jpn.* **7**, 722 (1992).
161. S. Noel, L. Boyer, and C. Bodin, "X-Ray Photoelectron Spectroscopy Investigation of Fluorocarbon Lubricant Films," *J. Vac. Sci. Technol. A* **9**, 32 (1991).
162. J. G. Newman and K. V. Viswanathan, "Purity and Thickness Analysis of Fluoropolymers by Static Secondary Ion Mass Spectrometry," *J. Vac. Sci. Technol. A* **8**, 2388 (1990).
163. Y. Hu and F. E. Talke, "A Study of Lubricant Loss in the Rail Region of a Magnetic Recording Slider Using Ellipsometry," *Tribology and Mechanics of Magnetic Storage Systems* **SP-25**, 43 (1988).
164. L. L. Nunnelley, M. A. Burleson, and G. G. Fuller, "On-Line Tribology Measurements on Lubricated Rigid Disks," *IEEE Trans. Magn.* **26**, 2679 (1990).
165. M. Yanagisawa, "Observation of Thickness Profiles on Lubricants During Sliding Tests," *Jpn. J. Appl. Phys.* **27**, L1609 (1988).
166. F. Levy and A. Wu, "The Preparation and Utilization of Radiolabeled Lubricants for Determining Lubricant Distribution on Magnetic Disk," *Tribology and Mechanics of Magnetic Storage Systems* **SP-16**, 49 (1984).
167. K. Tanimoto and E. Rabinowicz, "A Fluorescence Technique for Measuring Lubricant Thickness on Hard Magnetic Disks," *Tribol. Trans.* **35**, 537 (1992).
168. T. S. Sriram, K. J. Wahl, Y. W. Chung, B. Bhushan, and W. Rothschild, "The Application of Scanning Tunneling Microscopy to Study Lubricant Distribution of Magnetic Thin Film Rigid Disk Surfaces," *ASME J. Tribol.* **113**, 245 (1991).
169. G. S. Blackman, C. M. Mate, and M. R. Philpott, "Atomic Force Microscopy Studies of Lubricant Films on Solid Surfaces," *Vacuum* **41**, 1283 (1990).
170. W. H. McConnell, "On the Rate of Thinning of Thin Liquid Films on Rotating Disks," *J. Appl. Phys.* **64**, 2232 (1988).
171. M. Yanagisawa, "Depletion of Liquid Lubricants on Magnetic Recording Disks," *Tribology and Mechanics of Magnetic Storage Systems* **SP-22**, 93 (1987).
172. M. Yanagisawa, "Surface Migration and Lubrication Characteristics of Liquid Lubricants on Magnetic Thin Film Disks," *Tribology and Mechanics of Magnetic Storage Systems* **SP-27**, 101 (1990).
173. S. Kim, J. S. Kim, and F. Ma, "On the Flow of a Thin Liquid Over a Rotating Disk," *J. Appl. Phys.* **69**, 2593 (1991).
174. D. Peterson, "Long Spin Disk Lube Migration," *IEEE Trans. Magn.* **28**, 1988 (1992).
175. M. L. Forcada and C. M. Mate, "The Flow of Thin Lubricant Films on Rotating Disks," *Wear* **168**, 21 (1993).
176. F. Ma and J. H. Hwang, "The Effect of Air Shear on the Flow of a Thin Liquid Film on a Rough Rotating Disk," *J. Appl. Phys.* **68**, 1265 (1990).
177. R. G. Walmsley, B. R. Natarajan, and J. Brandt, "Effects of Temperature and Humidity on Thin Film Disk Lubricant Mobility," *IEEE Trans. Magn.* **29**, 3891 (1993).
178. V. J. Novotny and A. J. Marmur, "Wetting Autophobicity," *J. Colloid Interf. Sci.* **145**, 355 (1991).
179. M. L. Forcada and C. M. Mate, "Molecular Layering During Evaporation of Ultrathin Liquid Films," *Nature* **363**, 527 (1993).
180. I. Sugimoto and S. Miyake, "Ultraviolet-Light Irradiation of a Radio-Frequency Plasma Applied to Fluoropolymer Sputtering Deposition," *J. Appl. Phys.* **64**, 2700 (1988).
181. I. Sugimoto and S. Miyake, "Solid Lubricating Fluorine-Containing Polymer Film Synthesized by Perfluoropolyether Sputtering," *Thin Solid Films* **158**, 51 (1988).

Received November 16, 1995; accepted for publication May 28, 1996

Kenneth E. Johnson At the time this paper was prepared, Dr. Johnson was a senior scientist and manager of disk media development at the IBM Storage Systems Division laboratory in San Jose, California. Dr. Johnson received his B.S. in chemistry from Bates College in 1971, and his Ph.D. in physical chemistry from the University of Minnesota in 1977. After a year of postdoctoral work at the University of Chicago, he joined IBM in Rochester, Minnesota, to work on disk technology. Dr. Johnson was part of the team that developed IBM's first thin-film disk, shipped in 1988. He has been active in thin-film media topics, focusing on the magnetic and physical properties of thin films, and is the author of many papers on thin-film media and two book chapters describing disk technology.

C. Mathew Mate *IBM Research Division, Almaden Research Center, San Jose, California 95120 (mate@almaden.ibm.com).* Dr. Mate is a research staff member in the Storage Systems and Technology Department at the IBM Almaden Research Center. He received a B.S. degree in engineering physics in 1981 and a Ph.D. in physics in 1986, both from the University of California at Berkeley. Since joining IBM Almaden in 1986, he has studied tribology issues related to disk drive development and understanding how friction, lubrication, and wear occur at the atomic level. Dr. Mate has received several IBM awards for his work; he has coauthored 40 publications in scientific journals on the topic of tribology.

Jay A. Merz *IBM Storage Systems Division, 5600 Cottle Road, San Jose, California 95193 (jmerz@vnet.ibm.com).* Mr. Merz is an advisory engineer who is currently working on development of post-sputter processes. He received his B.S. degree in chemical engineering from Purdue University in 1980, and has been responsible for the development of a wide variety of disk processes since joining IBM in 1992. More recently, from 1988 through 1995, Mr. Merz has been responsible for texture process development. His focus has been on the effect of the process on head–disk tribology.

Richard L. White *IBM Storage Systems Division, 5600 Cottle Road, San Jose, California 95193 (RLWHITE at SJEVM5).* Dr. White is a senior engineer working in the Storage Systems Division. He has worked on projects ranging from magnetic bubble memories and magnetic film characterization to his current assignment in overcoat development for thin-film disks and thin-film disk tribology. He holds a B.S. in metallurgy and materials science from the University of Pennsylvania and a Ph.D. in materials science and engineering from Stanford University.

Anthony W. Wu Dr. Wu received his Ph.D. in chemistry from the University of Colorado in 1973. He joined IBM at San Jose as a postdoctoral fellow in 1975, and later transferred to the IBM East Fishkill, New York, facility as a staff engineer. In 1980, Dr. Wu returned to IBM San Jose, where he was involved in various phases of magnetic disk storage development. At the time this paper was prepared, he was a senior engineer at the IBM Storage Systems Division laboratory. Dr. Wu received five levels of IBM invention awards.